Laser-Scribed Photo-thermal Reduction of Graphene-Oxide for Thin Film Sensor Applications

By

Rouzbeh Kazemzadeh

M.Sc., Materials and Energy Research centre, Iran, 2009

Thesis Submitted in Partial Fulfillment of the
Requirements for the Degree of
Master of Applied Science

In the
School of Mechatronic Systems Engineering
Faculty of Applied Science

SIMON FRASER UNIVERSITY

Spring 2015

Approval

Name: **Rouzbeh Kazemzadeh**

Degree: **Master of Applied Science**

Title: ***Laser-Scribed Photo-thermal Reduction of Graphene-Oxide for Thin Film Sensor Applications***

Examining Committee: **Chair: Dr. Jason Wang**
Assistant Professor

Woo Soo Kim P.Eng
Senior Supervisor
Assistant Professor

Behraad Bahreyni P.Eng
Supervisor
Associate Professor

Ash Parameswaran P.Eng
Internal Examiner
Professor

Date Defended/Approved: April 24, 2015

Partial Copyright License

Abstract

In this thesis, a cost effective, simple and fast method of reduction of Graphene Oxide thin film is proposed. Graphene oxide is a non-conductive material intrinsically and one of the techniques to convert it to conductive material is using laser beam to remove oxygen groups from its surface, in other words, to reduce it. Laser parameters must be optimized for an effective and successful reduction. Thin film of non-conductive Graphene oxide is converted into conductive thin layer by fast laser scribing. Laser variables such as, power, speed, laser head distance to surface need to be selected precisely. Optical and atomic microscopies are used to study the changes of thin film surface. Chemical analysis shows that the reduction is successful and the structure is Graphene and removing of oxygen groups from surface is successful. Electrical properties also confirm the conductivity of scribed Graphene oxide.

To show the application of reduced Graphene oxide, laser scribing method is used to fabricate pressure sensors arrays and the final product shows acceptable sensitivity to light touches similar to scrolling with finger on a touch screens. The fabricated sensor array is attachable on any surface for monitoring applied forces or pressure and maintains good electrical conductivity under mechanical stress and thus holds promise for durable sensors.

Beside the pressure sensor, reduced Graphene oxide thin film has been used to fabricate temperature sensor. Also thin layer of hybrid (Graphene oxide mixed with silver nano wire) is deposited and patterned in the form of interdigitated capacitor to test the capacitance change of touch sensor.

Keywords: Reduced Graphene Oxide, Laser scribing, touch sensor, temperature sensor, thin film.

To my Family

Acknowledgements

First of all, I would like to give my best acknowledgement to my senior supervisor Dr. Woo Soo Kim. Under his supervision, I have learnt a lot about efficient management and execution of my work. Moreover, he always encourages me to think big and try my ideas even if they do not sound that practical initially. I also would like to give special thanks to my supervisory committee members, Dr Parameswaran and Dr Bahreyni for their willingness to read my thesis and for the valuable suggestions. I appreciate your input that improved my thesis in many ways.

Second of all, I deeply appreciate my friends in Stretchable Devices Lab for firmly supporting me in terms of study, work and life all the time. In particular, Jiseok Kim is such a nice friend. He contributed so much to my research and he is willing to spare time from his doctoral study to discuss with me. Also, I would like to thank Kimball Andersen for his helpful ideas and suggestions.

Most importantly, my deeply loved family are like the brightest stars in the sky, which rejoice and inspire me to move forward when I am walking alone in the darkness. Forever love to my family.

Table of Contents

List of Tables

List of Figures

List of Acronyms

AFM	Atomic Force Microscopy
AgNPs	Silver Nano Particle
AgNW	Silver Nano Wires
CVD	Chemical Vapor Deposition
DCT	Graphene-on-Demand by Cut-and-choose Transfer-printing
DMAc	DiMethylAcetamide
DMF	Dimethyl Formamide
DMSO	Dimethyl Sulfoxide
EBL	Electronic Beam Lithography
EDLC	Electrical Double-Layer Capacitor
EDX	Energy-Dispersive X-ray spectroscopy
EG	Ethylene Glycol
FLG	Few Layer Graphene
FTIR	Fourier transform infrared spectroscopy
GO	Graphene Oxide
GO-AgNW	Graphene Oxide Silver Nano Wire
IGO	Improved Graphene Oxide
ITO	Indium Tin Oxide
LCR	Inductance (L), Capacitance (C), Resistance (R)
mNW	metal Nano-Wires
NMP	N-MethylPyrrolidone
OLED	Organic Light-Emitting Diodes
OTFT	Organic Thin Film Transistor
PET	Polyethylene terephthalate
PDMS	Polydimethylsiloxane
PMMA	Poly Methyl MethAcrylate
PVA	Poly Vinyl Alcohol
RFID	Radio frequency Identification
r-GO	Reduced Graphene Oxide
RTD	Resistance Temperature Detectors
RTP	Rapid Thermal Processing

SEM	Scanning Electron Microscopy
TCR	Temperature Coefficient of Resistance
TFT	Thin Film Transistor

Chapter 1

Introduction

Manipulation of properties of materials, especially enhancing the electrical properties of materials is of great importance in organic electronics. Unlike the common inorganic conductors and semiconductors, organic electronics are based on organic (carbon-based) and polymer molecules. One of the main benefits of such devices is their low cost compared to conventional ones [1]. In this regard conformable circuits and electronics are highly desirable. One of the new organic structures that have potential application in organic electronics is Graphene [1]. It is a newly discovered material and attracted scientists and academic attentions worldwide. So it is worth to study about manipulating of its electrical properties.

1.1. Motivation

The focus of projects in our research group - Stretchable Devices Lab (SDL) - is developing flexible electronics, e.g., FETs, RFID's. In more detail, major activities are development of micro/nano-scale manufacturing and integration to investigate engineering challenges for smart, stretchable, robust applications and biomimetic materials with a wide range of research projects in the field of nano structures and solution phase materials. Considering the potential use of Graphene in fabrication of organic electronics and considering the scope of SDL lab, Graphene oxide has been chosen. Unique properties of Graphene encouraged us to define a project on studying and developing electronics based on Graphene. Also we tried some novel methods to enhance its electrical properties. At the beginning, the project is about chemical reduction of Graphene oxide solution but later it is found that the chemical reduction did not deliver high quality products. Thermal reduction has been considered as next option.

After shining laser beam on thin film Graphene oxide, very interesting results came up and laser writing has been selected as a simple, fast and solution free method.

1.2. Objectives

The objective of this project can be summarized as:

- Effective photo-thermal reduction of Graphene oxide by laser beam
- Patterning of thin film sensor designs in-situ by laser scribing
- Confirmation and Analysis of reduced Graphene oxide using optical, chemical, and electrical methods
- Demonstration of thin film Graphene-based sensors for printed sensor applications

1.3. Contribution

The main contributions of this thesis can be summarized as:

- Enhancing the electrical properties of Graphene oxide by reducing it using laser beam.
- Proposing a unique method of fabrication for the first time which can be further modified for better final products.
- Offering fast, simple and solution free reduction of Graphene oxide, which is very important for mass production.
- Optimization of CO_2 laser beam parameters exclusively for scribing and patterning of thin film Graphene oxide on Polyethylene terephthalate (PET).
- Fabrication of touch sensors using only Graphene.

Published paper:

- R. Kazemzadeh, K. Andersen, L. Motha and W.S. Kim*, “Highly Sensitive Pressure Sensor with Reduced Graphene Oxide” IEEE Electron Device Letters 36, pp.180-182 (2015).

Peer Reviewed Conference Proceedings/Papers:

- R. Kazemzadeh, and W.S. Kim*, “Flexible Temperature Sensor with Laser Scribed Graphene Oxide”, Proceeding of IEEE Nano, TuDPS.20, August 2014
- R. Kazemzadeh, and W.S. Kim, “Fast Fabrication of Graphene-Based Sensitive Pressure Sensors Using Laser” LL6.10, MRS 2015 proceeding.

1.4. Thesis organization

Remain of the thesis is structured as follows. Chapter 2 provides background and literature review of Graphene, production method, patterning and applications in electronics. Chapter 3 describes our fabrication method, selection of laser parameter, scribing of thin layer and sensor fabrication. Chapter 4 explains our characterization methods, analysis and results. Chapter 5 concludes the thesis and outlines future work.

Chapter 2

Graphene background

2.1. Overview

Carbon is the most abundant element in organic compounds. The ability to transfer electrical current and its flexible structure let it to form a lot of different structures with large variety of physical properties.

Among molecules with only carbon atoms, Graphene, has been introduced to the world since 2004 [2]. In 1947 *P. R. Wallace*, predicted that Graphene should have extraordinary electronic properties [2]. The name “Graphene” first was used in 1987. It is believed that Graphene can change the world because it has applications in so many different areas. It can be isolated simply by putting some graphite between pieces of Scotch tape and peeling it off a few times. Andrei Geim and Kostya Novoselov rewarded with Nobel Prize in physics on December 10, 2010 for the discovery of Graphene [2].

Numerous papers have been published since the first time introduction of this new carbon structure in 2004, just in *sciencedirect.com* a quick search for the papers with the “Graphene” in the title, returns 8,679 papers from 2004 till 2014. Figure 2-1 shows how it has been popular during ten years period. By looking at the graph, we can see the numbers are doubled from 2012 to 2014. This shows, how important is research on this unique material.

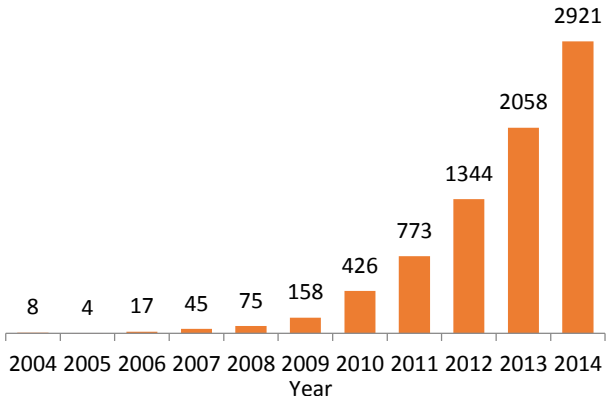

Figure 2-1. Number of papers with “Graphene” in the title from 2004 to 2014

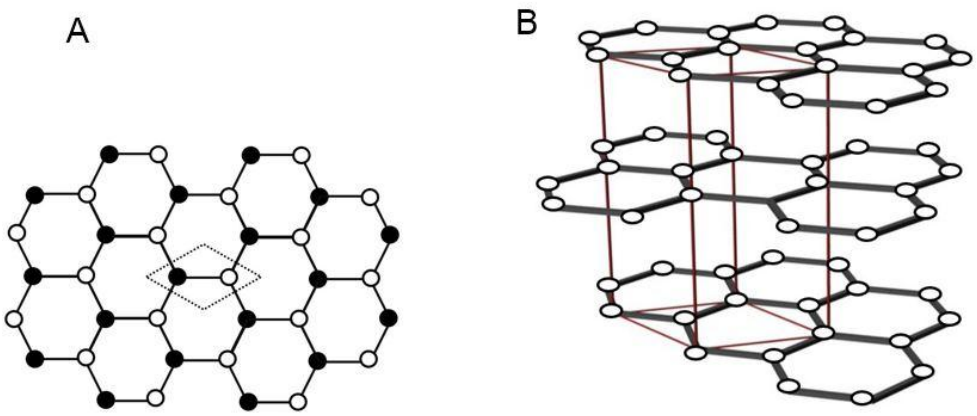

Figure 2-2. The structures of (A) Graphene (B) Graphite. The unit cell of Graphene has two independent carbon atoms (filled and open circles)

2.1.1. Structure

Graphene is a thin monolayer of sp^2-bonded carbon atoms as "two-dimensional structure” made of hexagonal rings. Graphene structure is arranged in a honey-comb lattice (Figure 2-2). For Graphene, it has been shown that the electronic structure changes with the number of layers; it approaches the 3D limit of graphite at 10 layers [6]. Some of the unique physical properties of Graphene is extreme mechanical strength, exceptionally high electronic and thermal conductivities, impermeability to gases and very high intrinsic mobility [4]. Graphene is the basic structural element of some carbon allotropes including graphite, carbon nanotubes and fullerenes [5].

Before discovery of Graphene and other 2D molecules (for example, single-layer boron nitride) it is believed that 2D structures are thermodynamically unstable and cannot exist. These crystals have grown on top of non-crystalline substrates, in liquid suspension. 2D crystals also have exhibited high crystal quality. For example in the case of Graphene, electrons can move long interatomic distances without scattering [2].

Lattice constant of unit cell of Graphene is a = 0.246 nm, it is formed of two independent carbon sites, where the strong σ-bonds and weak π- bonds of the carbon atoms give a bond length of 0.142 nm [6].

2.2. Types of Graphene

Graphene comes in different forms like, few layer Graphene, Graphene oxide and reduced Graphene oxide (r-GO). Each has its own properties and applications.

Few layers Graphene (FLG): Also called multi-layer Graphene is a free standing flake, consisting of 3 to 10 stacked Graphene layers of extended lateral dimension; FLG is good for composite materials and for mechanical reinforcement [7].

Graphene oxide (GO): Type of Graphene prepared by exfoliation and oxidation. Graphene oxide is a monolayer material with high oxygen content [8].

Reduced Graphene Oxide (r-GO): Graphene oxide which is reduced by chemical, thermal, microwave, photo-chemical, photo-thermal, microbial or laser to reduce its oxygen content. Conductive inks, sensors and electronics are potential use for r-GO [9] .

2.3. Properties of Graphene

Each material is identified by its physical, electrical and mechanical properties. Uniqueness of Graphene is because of its extreme properties reaching theoretical prediction limit. Electron mobility is defined as: how fast an electron can move through a metal or semiconductor, when an electric field presented [10]. Room-temperature electron mobility of Graphene is 2.5×10^5 cm^2V^{-1} s^{-1} which is extremely high [2].

Young's modulus is a measure of the stiffness of an elastic material. It is defined as the ratio of the stress (force per unit area) along an axis to the strain along that axis in the range of Hooke's law [11]. Graphene has Young's modulus of 1 TPa and strength of 130 GPa (very close to the value that predicted by theory).

A band gap or energy gap refers to the energy difference (in electron volts) between the top of the valence band and the bottom of the conduction band in insulators and semiconductors [12]. Graphene and its bilayer have simple electronic spectra: they are either zero-gap semiconductors or semi-metal with one type of electron and one type of hole. For three or more layers, the spectra become very complicated: The conduction and valence bands start to overlap. This allows single, double and few (3 to 10) layer Graphene to be distinguished as three different types of 2D crystals [2]. Thermal properties of Graphene are also interesting. Graphene has very high thermal conductivity (above 3,000WmK^{-1}) [13].

2.4. Preparation of Graphene

2.4.1. Chemical Vapor Deposition based Graphene

Graphene is produced using several different methods:

- Graphene grown on silicon carbide [14].
- Mechanical exfoliation from graphite [15].
- Reduction of exfoliated graphite oxide and green approach through electrochemical reduction of exfoliated graphite oxide [16], [17].
- Laser-Induced reduction of Graphite oxide [14].
- Growth by chemical vapor deposition (CVD) on metal surfaces [19], [20].

CVD is an important method for the production of high quality high performance Graphene for a variety of applications. This method has been reported in 2008 for production of Graphene [21]. In CVD method, the substrate is exposed to one or more volatile precursors, which react and/or decompose on the substrate surface to produce

the desired deposit. Exhaust by-products are removed by gas flow from the reaction chamber [22]. Different components of a CVD apparatus are:

- Gas delivery system and the supply of precursors.
- Reactor chamber which is basically furnace.
- Substrate loading mechanism.
- Vacuum system for removal of all exhaust gaseous species after completion of reactions.
- Exhaust system for removal of volatile by-products.
- Process control equipment like gauges, controls etc. to monitor process parameters such as pressure, temperature and time [23].

A general schematic of synthesis of Graphene using CVD method is shown in Figure 2-3.

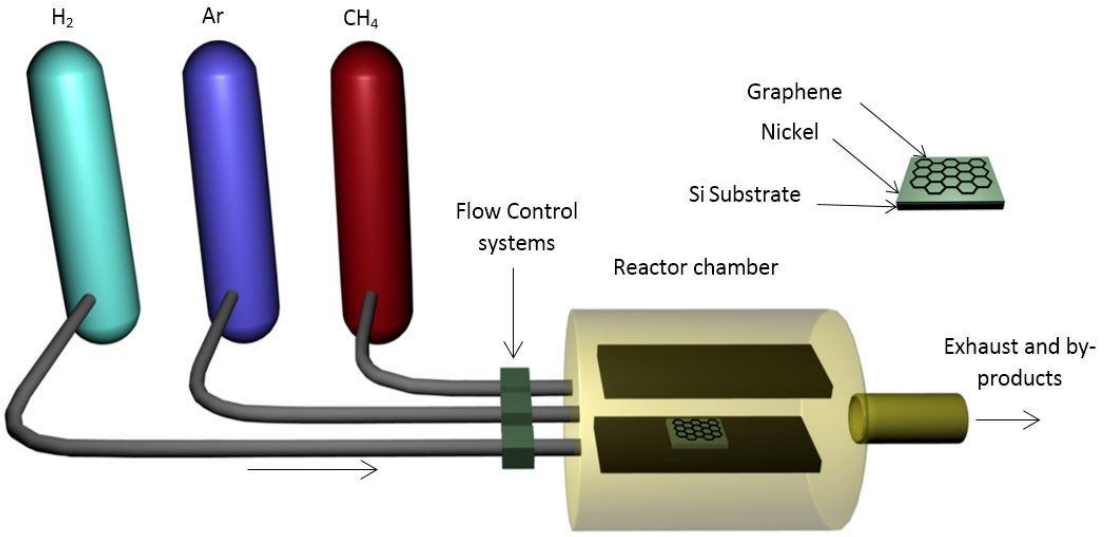

Figure 2-3. Schematic of CVD apparatus for synthesis of Graphene

Chemical vapor deposition on single crystal transition metals has shown to be capable of covering relatively high area with high quality Graphene. However; substrates being used are expensive and inhibit the use of this method in large-scale processes. Recently, other less expensive and more feasible methods for CVD synthesis of high quality large area Graphene are offered using nickel and copper films and foils [19]. Here we look at these methods in more details.

The CVD preparation of Graphene on Nickel is a two–step process. First, carbon atoms incorporate into Ni substrate, second those carbon atoms diffuse onto Ni surface to form Graphene layers while the substrate is cooling quickly [25].

It starts with annealing of polycrystalline Ni films in Ar/H_2 at 900-1000°C. This is done for increasing grain size of Ni. Then, films are exposed to H_2/CH_4 mixture. In this step, Methane gas decomposes and carbon atoms dissolve into the Ni film to form a solid solution. Finally, films are cooled down in argon gas [21]. Figure 2-4 shows the mechanism of Graphene formation on nickel surface. It has been reported that using a cold-wall reactor with a rapid thermal processing (RTP) heater provide a fast heating & cooling rate and temperature control which is benefit to CVD-grown Graphene since the temperature is main parameter on the number of layers, thickness uniformity and quality of Graphene film. Furthermore decreasing H_2 concentration increases the quality of Graphene films dramatically. Without presence of H_2, the Graphene film has a sheet resistance of ~367 Ω/□ [26].

Microstructure of Nickel substrate has an important role in morphology of produced Graphene film. Nucleation of multi-layer occurs at the grain boundary of Ni. It is believed that annealing of Ni substrates at elevated temperatures in hydrogen atmosphere not only increases single-crystalline Ni grain size but also improves the Graphene quality [21].

After growing of Graphene, it needs to be transferred to a different target substrate. First a mixture of PMMA in chlorobenzene is spin-coated onto the as-grown Graphene. Then PMMA/Graphene/Ni foil is cured and subsequently, the rear side of the Ni foil is polished to remove the coatings by chemical etching of Ni with a $FeCl_3$.The floating PMMA supported- Graphene is transferred onto arbitrary substrates such as a SiO_2/Si substrate. Finally, PMMA is dissolved in acetone, leaving Graphene on a target substrate [27].

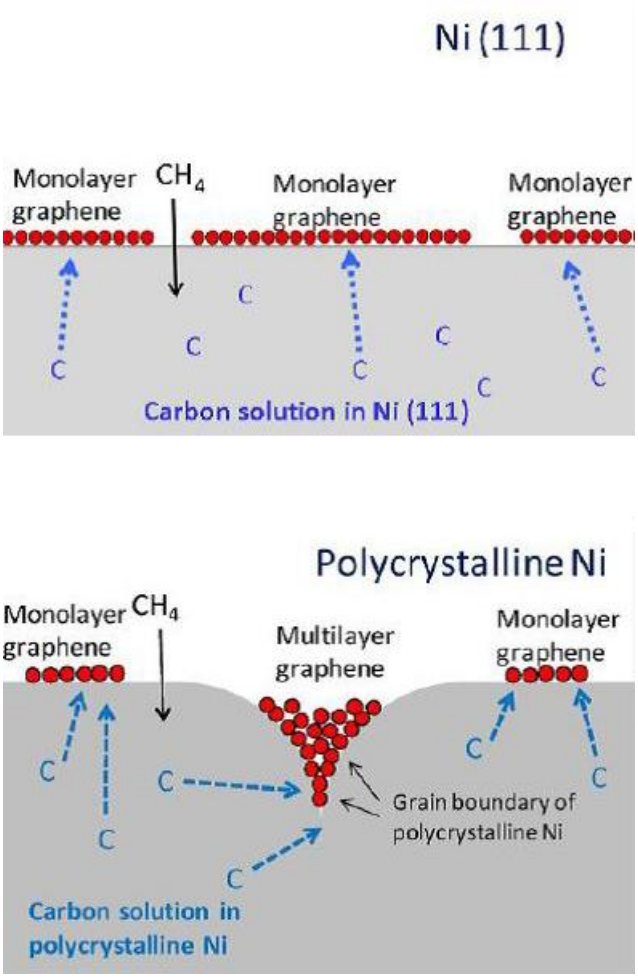

Figure 2-4. Graphene growth mechanism on Ni (111) and polycrystalline Ni surface [21].Reprinted with permission.

Beside nickel, scientists have tried to grow Graphene on other metal layers such as Cu, Ir, Pt, Co, Ru, Pd, and Re. These metals show different carbon solubility. In case of the growth on copper surface a well-known method is proposed by Ruoff et al., in this method Graphene films have grown on micro meter thick Cu foils in a hot wall furnace. First the Cu foil is heat treated in hydrogen at 1000°C, and then the typical Hydrogen – Methane mixture is introduced into the chamber to begin the Graphene growth. After forming a Graphene layer on Cu foil, the chamber is cooled down to room temperature. Formation of Graphene can be confirmed by Raman Spectroscopy.

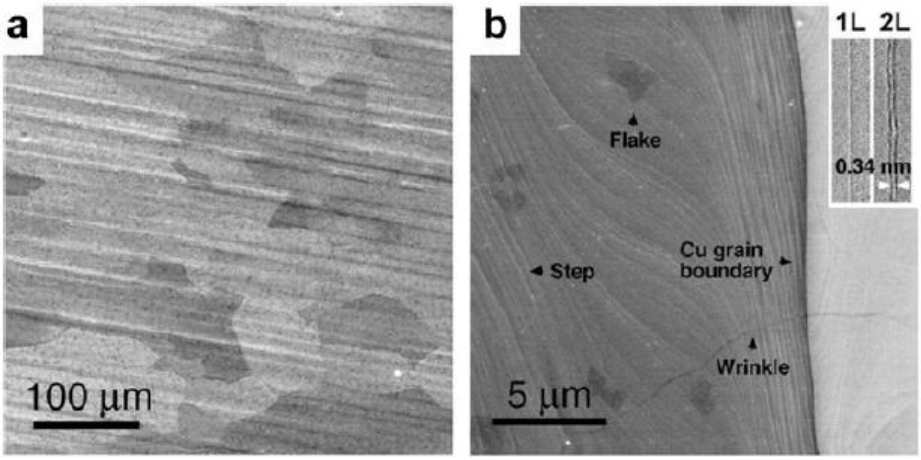

Figure 2-5. (a) SEM image of Graphene on a copper foil. (b) High-resolution SEM image of Graphene on Cu [21]. Reprinted with permission.

Figure 2-5a, shows SEM image of Cu grains. Figure 2-5b shows more details. The darker areas are multiple-layer Graphene. Graphene “wrinkles” originate from the different thermal expansion coefficient of Graphene and Cu. Those wrinkles can go across Cu grain boundaries. As Figure 2-5b shows, the Graphene film is continuous. Graphene grown on Cu foil can be easily transferred to other substrates such as glass for further study [21].

Comparing the growth of Graphene on Ni and Cu, shows that growth parameters such as film thickness and cooling rate have little influence on Graphene CVD growth on Cu. The analytical comparison is demonstrated in Figure 2-6. From the optical image of Graphene (Figure 2-6b and d), it is obvious that Graphene grown on Ni has many multilayer flakes while Graphene on polycrystalline Cu is uniform monolayer (Figure 2-6 d).

For Graphene formation on Ni, segregation process has been suggested for growth mechanism (Figure 2-6a), that means suppression of multilayer formation is difficult. In contrast, Cu has really low carbon solubility. The carbon for formation of Graphene comes from the hydrocarbon, which decomposes catalytically on the Cu surface (Figure 2-6c). When the copper layer is covered with first layer of Graphene, there is no catalyst exposed to hydrocarbon to promote decomposition and growth. Thus, the Graphene growth on Cu is a surface reaction process, which is self-limiting and robust [21].

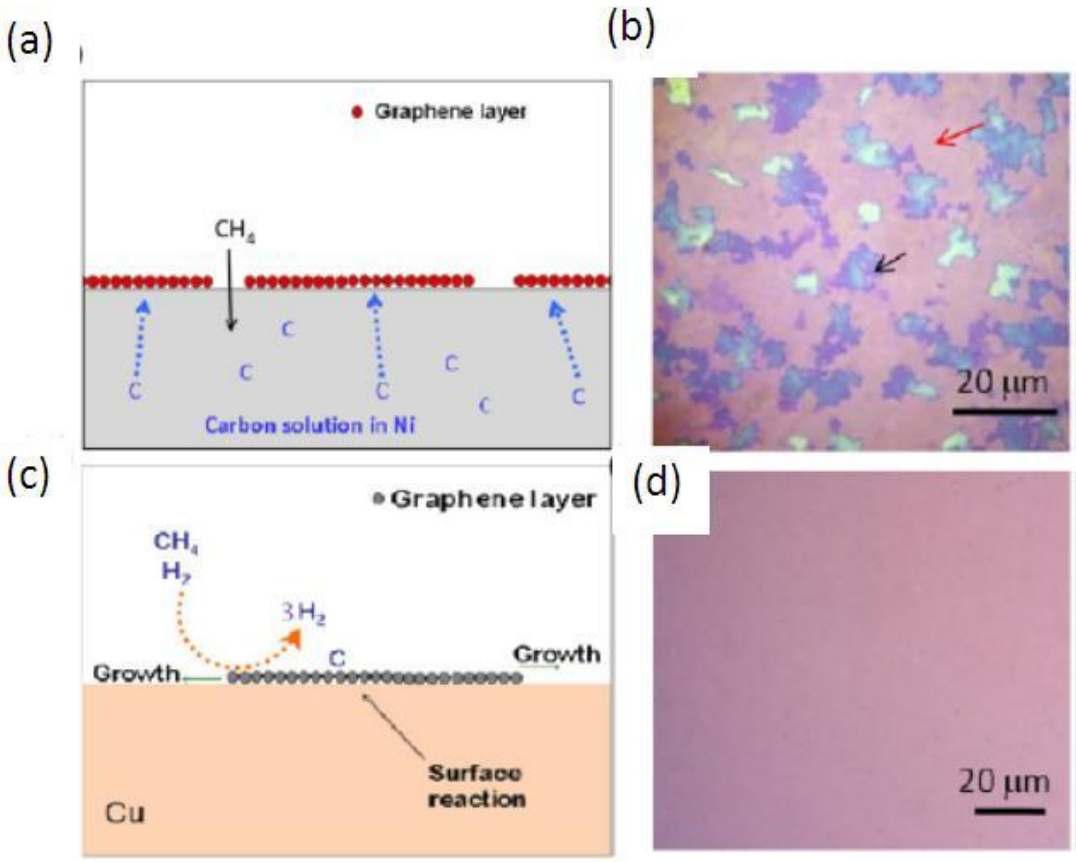

Figure 2-6. Schematic diagrams of Graphene growth mechanism on Ni (a) and Cu (c). Optical images of Graphene transferred to SiO_2/Si substrates from Ni substrate (b) and Cu substrate (d) [21]. Reprinted with permission.

2.4.2. Solution-based Reduced Graphene Oxide

A common issue in the described CVD technique is the use of metal substrates which often necessitates a transfer of the Graphene onto other substrates. A possible solution to overcome the above problems is the use of solution based techniques to separate the layers of graphite thus yielding a suspension of Graphene. There have numerous approaches explored in this regard, all of which follow the same underlying principle of liquid phase exfoliation by weakening the Van der Waals interaction between the layers of graphite by either intercalation or functionalization of the individual layers. This approach is both scalable, affording the possibility of high-volume production, and provides versatility in terms of being well-suited to chemical functionalization. Therefore it is promising for a wide range of applications.

Graphite intercalation compounds are interesting starting materials to obtain colloidal dispersions of single layer Graphene sheets. This approach should allow the production of high quality single layer sheets of Graphene. Colloidal suspensions of Graphene sheets in organic solvents such as N-methylpyrrolidone (NMP) are obtained by sonication of graphite powder, however, only with lateral sizes of a few hundreds of nanometers and quite low yield [28].

There are many other methods and recipes for stable suspension of Graphene by exfoliation are solution. One of the widely used one is reduction of graphite oxide or oxidized layers of graphite. A major advantage of the graphite oxide approach to Graphene is that it is straight forward to synthesize, process, and integrate into devices using existing top down approaches of thin film electronics technology. This method offers potential for the production of chemically derived Graphene on an industrial scale. [29]. Figure 2-7 shows the different steps in exfoliation of graphite oxide [30].

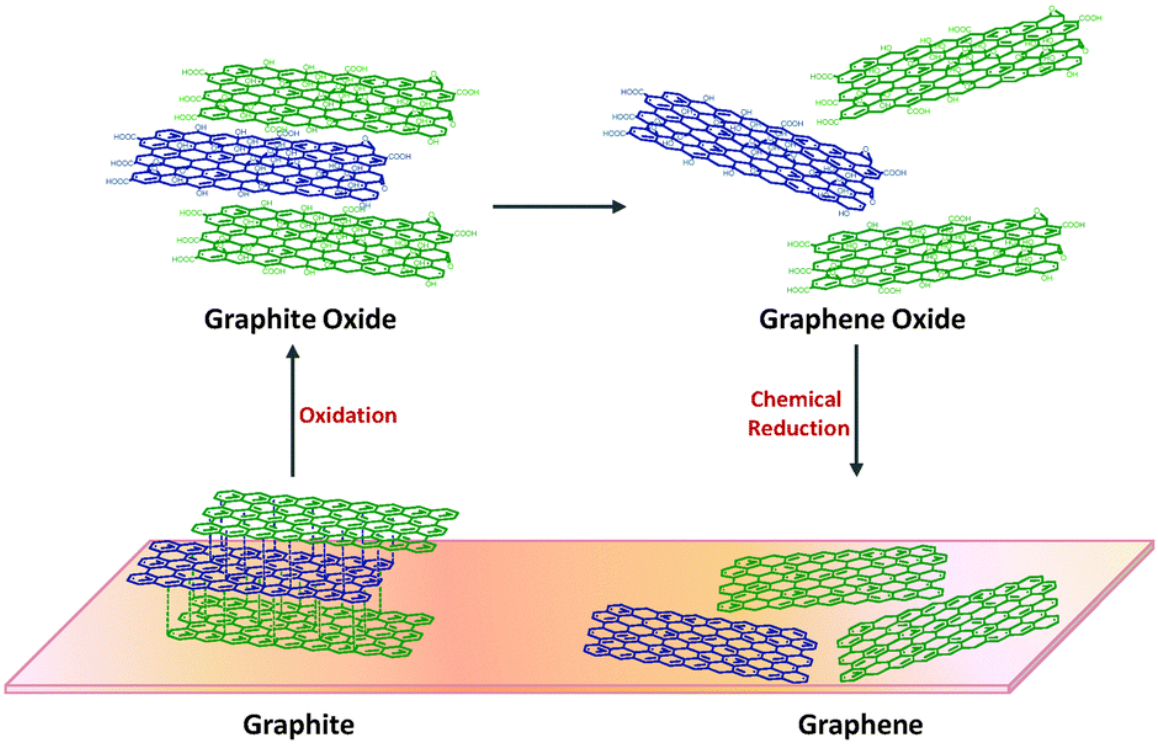

Figure 2-7. Schematic of exfoliation of Graphite oxide [30]. Reprinted with permission.

A very famous synthesis method of graphite oxide is reported by the Brodie [32] and Hummers [33]. The Hummers method uses a combination of potassium permanganate ($KMnO_4$) and sulfuric acid (H_2SO_4). Although permanganate is a well-established oxidizing agent, the active species in the oxidation of graphite is di-manganese heptoxide (Mn_2O_7), which appears as brownish red oil formed from the reaction of $KMnO_4$ with H_2SO_4 (Eq. (1) & (2)).

$$KMnO_4 + 3H_2SO_4 \rightarrow K^+ + MnO_3^+ + H_2O^+ + 3HSO_4^- \quad (1)$$

$$MnO_3^+ + MnO_4^- \rightarrow Mn_2O_7 \quad (2)$$

Graphite oxide synthesized by this method exists in as a brown viscous colloid, which contains not only graphite oxide but also non-oxidized graphitic particles and the residue of the reaction by-products [9] , [34].

An improved Hummers method for producing Graphene Oxide (GO) shows significant advantages over Hummers' method. It is found that excluding the $NaNO_3$, increasing the amount of $KMnO_4$, and performing the reaction in a different ratio of H_2SO_4 to H_3PO_4 improves the efficiency of the oxidation process. This method provides a greater amount of hydrophilic oxidized Graphene material as compared to Hummers' method [35]. Figure 2-8 shows the steps of improved Hummers method. The increased efficiency of the IGO (improved GO) method is indicated by the very small amount of under-oxidized material produced.

Although GO itself is non-conductive, its carbon framework can be restored by thermal treatment or treatment with chemical reducing agents resulting in reduced Graphene Oxide (r-GO). Earlier efforts mainly involved the use of hydrazine vapor for this purpose. However hydrazine is very toxic and explosive. Figure 2-9 shows the SEM images of r-GO prepared using hydrazine [36].

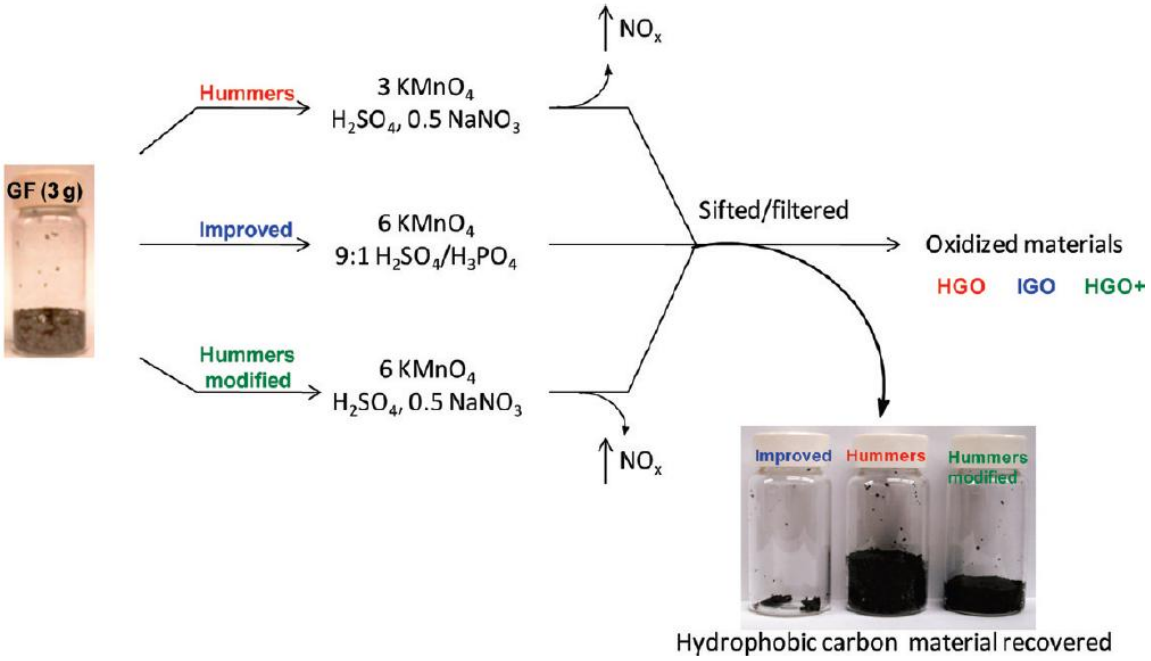

Figure 2-8. Steps of improved Hummer method [35]. Reprinted with permission.

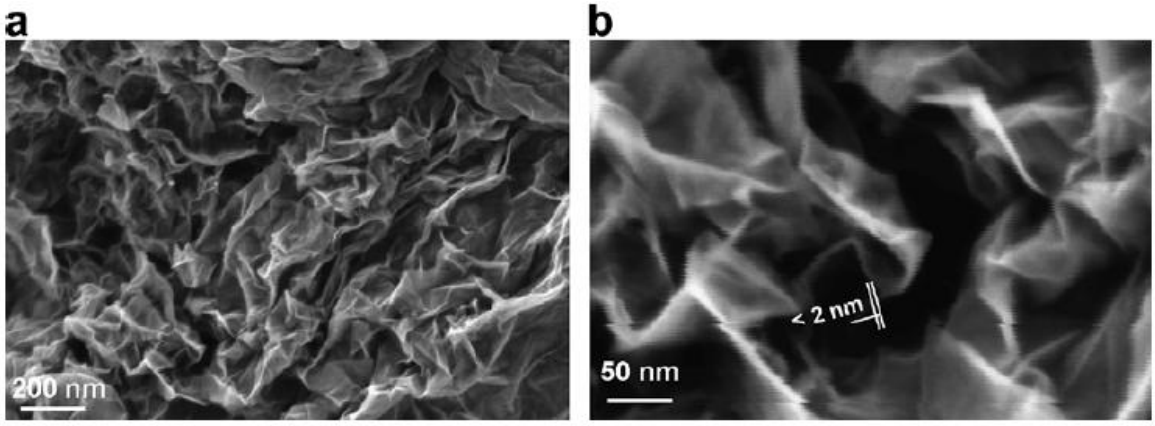

Figure 2-9. (a) An SEM image of aggregated reduced GO sheets. (b) A platelet having an upper bound thickness at a fold of 2 nm [36]. Reprinted with permission.

SEM images shows that the r-GO consists of randomly aggregated, thin, crumpled sheets closely associated with each other and forming a disordered solid (Figure 2-9 a). The folded regions of the sheets (Figure 2-9 b) are found to have average widths of 2 nm [36].

Briefly Hydrazine hydrate is added and the Graphite oxide solution heated in an oil bath at 100°C under a water-cooled condenser for 24h over which the reduced GO

gradually precipitated out as a black solid. This product is isolated by filtration over a medium fritted glass funnel, washed with water and methanol, and dried on the funnel [36].

Several safer alternative materials have been explored. Sodium borohydride ($NaBH_4$) has been demonstrated to function more effectively than hydrazine as a reductant of GO. Sodium borohydride hydrolysis is slow in water, but function effectively as reductants of GO, in this method the sheet resistance of $NaBH_4$-reduced films is much lower than that of hydrazine-reduced film [37].

Other works suggest that some compounds containing sulfur such as $NaHSO_3$, Na_2SO_3, $Na_2S_2O_3$, $Na_2S{\cdot}9H_2O$, $SOCl_2$, and SO_2, are used as reducing agents to reduce Graphene oxide. $NaHSO_3$ and $SOCl_2$ show similar reducing ability like Hydrazine. $NaHSO_3$ is a better reducing agent for GO with less harm. The electrical conductivity of the Graphene paper prepared using a $NaHSO_3$ is 6500 $S.m^{-1}$, while it is 5100 $S.m^{-1}$ for hydrazine-reduced Graphene paper [38].

2.4.3. Thermal and Solvothermal Methods

It has been shown that Graphene oxide thin films can be reduced by heat treatment in ultra-high vacuum or a reducing environment at high temperatures of 900–1000°C [39]. Therefore reduction in lower temperature still is a challenge. In one work, synthesis and reduction of Graphene oxide platelets deposited on Si_3N_4/Si substrates have been investigated. Nearly no functional group bonds have been observed at the high temperature of 1000°C in the one-step reducing procedure. By applying the two-step reducing procedure at low temperatures of ≤500°C, similar high quality Graphene thin films are obtained [40].

Solvo-thermal methods are another practical approach to prepare Graphene. In one attempt rapid and mild thermal reduction of GO to Graphene is achieved with the assistance of microwaves in a mixed solution of N, N-dimethyl acetamide and water ($DMAc/H_2O$). The mixed solution can be used as solvent for the produced Graphene and at the same time this medium can be used as the reactive system for microwave treatment and also as a thermal reservoir to control the temperature of the system up to

165°C. The yield of product prepared by this method is high and production of gram level is easily achieved [41].

Other groups have tried different solvent mixtures in solvo-thermal approach to investigate the effect of solvent. It is found that carboxylic groups and carbonyl groups are decomposed between the temperatures of 100 and 150 °C. The solvent used to disperse GO can assist the decomposition reaction. The solvents used are H_2O, *N*,*N*-dimethyl formamide (DMF), ethylene glycol (EG) and dimethyl sulfoxide (DMSO).The interaction between solvent molecules and functional groups promotes the diffusion rate of epoxy groups and plays an important role in the reaction. Different solvents show different abilities in assisting this reaction. However, the catalytic mechanism is still not clear because of the limitation of the solvents that can be used in our study. At 150 °C, DMF accelerates the GO reduction rate significantly, while dimethyl sulfoxide (DMSO) has less acceleration effect [42].

2.5. Hybrid Carbon Materials

Indium tin oxide (ITO) is the most commonly used material for transparent electrodes, but some of the material properties especially its brittleness and price limit its functionality for flexible devices. Thus, there is a need for new transparent conductive materials with better mechanical properties. Proposed alternative materials are conductive polymers, carbon nanotubes, Graphene, nanowires and metal mesh-structures. Graphene and percolating networks of metal nanowires (mNW) have been considered as promising candidates because of combined mechanical flexibility and high electrical conductivity. Charge transport occurs along distribution of NWs with random orientations. Some disadvantages of mNW, such as:

- Low overvoltage threshold
- High wire to wire junction resistance
- High contact resistance between the network and active materials
- Material instability
- Poor adhesion to plastic substrates

Limit their application. Graphene-mNW hybrid structures as conductive, transparent, and stretchable electrodes allow charge transfer in the hybrid nanostructure, each complementing the disadvantages of the other component. Metal wire network can be Silver nanowires (AgNW). Graphene adsorption at inter-wire junctions can enhances electrical properties by several orders of magnitude [43], [44], [45], [46]**.** In one application Graphene oxide is used as a kind of soldering material to join silver nanowire percolation network [47].(Figure 2-10).

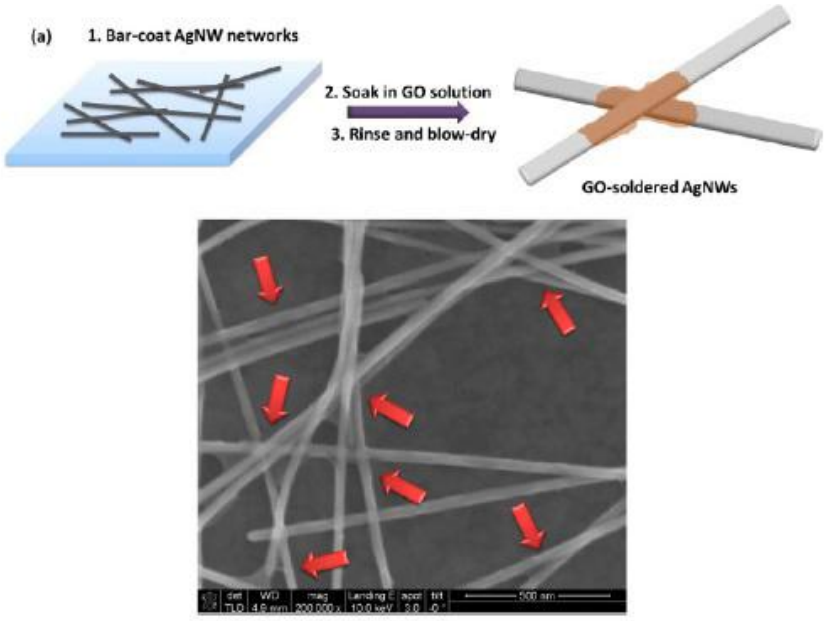

Figure 2-10.Fabrication of a GO-AgNW network and GO-soldered AgNW [47]. Reprinted with permission.

Different arrangement of layers has shown to be effective in terms of better conductivity and durability. Reduced Graphene oxide/silver nanowire/polymer stacked layers shows very low sheet resistance and high transparency. Figure 2-11 shows the different steps of fabrication of the stacked layers. (4.0 Ω/☐ sheet resistance and a 75% diffuse transmittance). The film possessed a much wider transparent wavelength region than only ITO. The reduced Graphene oxide film has prevented corrosion of the silver nanowires [48].

Other hybrid nanostructures based on Graphene and metal nano-trough networks are used as stretchable and transparent electrodes. Compared to the single

material of Graphene or the nano-trough, a very low sheet resistance (1 Ω/☐) as well as high transparency (91% in the visible light range), and excellent stretchability (80% tensile strain) is reported for the hybrid structure.

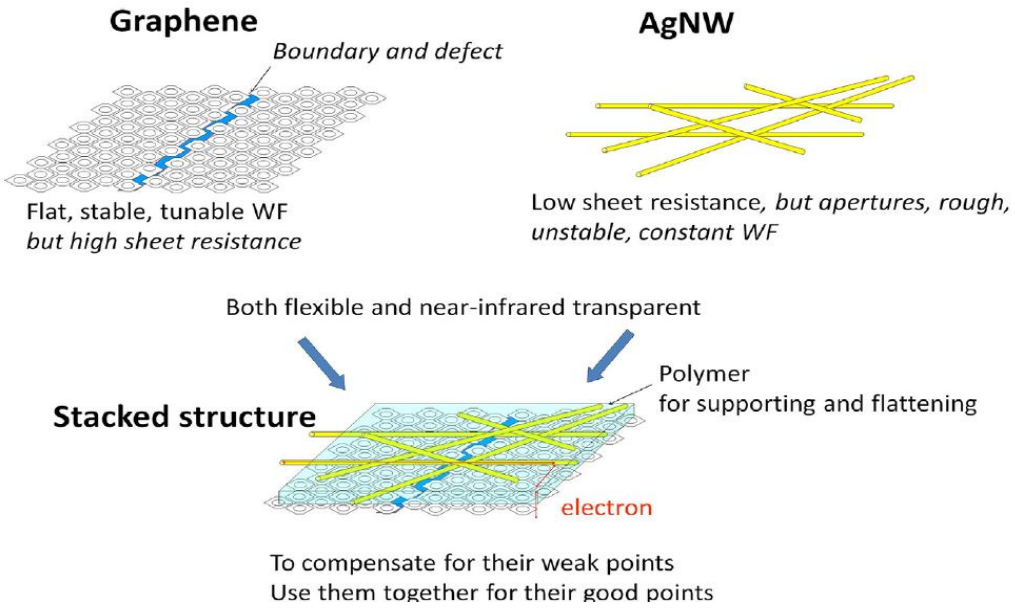

Figure 2-11. Arrangement of conductive transparent Graphene/ (AgNW)/polymer stacked layers [48]. Reprinted with permission.

The fabrication steps for this kind of structure can be summarized as below:

- Nanofiber webs of a poly vinyl alcohol (PVA) are produced on a collector by electrospinning.

- After deposition of metal (100 nm of Au) onto the upper side of the free-standing fibers, the lower surface (polymer side) of the fiber, where the metal is uncoated, is placed in contact with the desired substrate.

- Removing the polymeric sacrificial template using solvent, left only the nano-trough with a thin, convex, half-shell cross-section on the substrate. The steps are shown in Figure 2-12 [49].

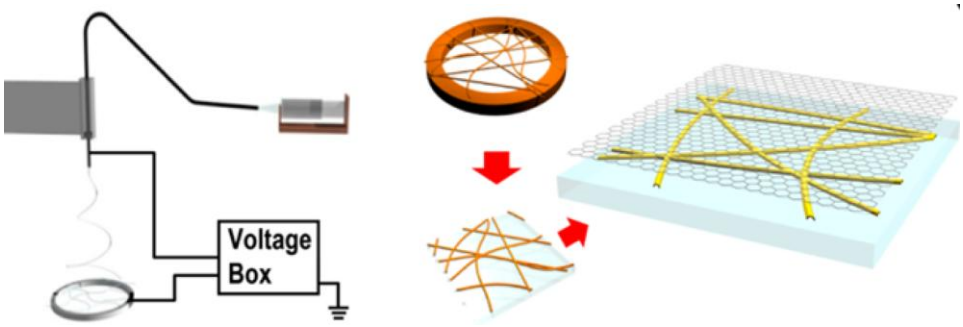

Figure 2-12. Schematic of nano-trough fabrication [49]. Reprinted with permission.

It is believed that silver nanowires prevents Graphene sheets from restacking and aggregation after reduction from Graphene oxide, increasing the electrical conductivity between the Graphene layers [50]. Using metal nano particles and Graphene composite also has been reported [51].

In general the combination of Graphene (or Graphene oxide) and metal nano wires (or metal nano particles) is beneficial because the Graphene sheet is a useful material to solder AgNW junctions. The highly conductive and transparent GO-AgNW networks can be formed on flexible substrates such as PET via an all solution- based process at room temperature. GO-AgNW networks exhibit high mechanical flexibility.

2.6. Patterning of Graphene Materials

Properties of pristine Graphene makes it such a unique substance but in order to harness its potential semiconducting properties we should be able to fine tune and control its behaviour as well. The key to employ the Graphene as industrial future material is to accurately tune its conductivity by doping or pattering by feasible steps. Graphene is a semimetal and direct application of it in electronic devices is difficult. In various processes the amount of energy which is involved in tailoring Graphene is different. One approach is breaking C – O bonds selectively, which can be achieved by irradiation with energetic electrons, laser, chemical reactions, or high temperature treatment [52].

In case of GO the patterning is completely necessary because it is not conductive at all and needs to be conductive at select areas depending on the device design. Several methods have been used to pattern Graphene or Graphene oxides:

- Direct mechanical cleavage [53], [54].
- Electron beam irradiation [55].
- Scanning probe lithography [56].
- Helium ion beam lithography [57].
- Photo-catalytic etching [58].
- Plasma etching [59].
- Chemical etching [60].
- Nano-imprint lithography [61].
- Reduction of Graphene oxide [62].

2.6.1. Printed Graphene

Inkjet-printed Graphene is an industrial method to manufacture large-area and flexible electronics. It is applicable to make touch screens, sensors, electronic paper (e-paper), radio frequency tags, and electronic textiles. A range of components can be printed, such as transistors, photovoltaic devices and displays [63].

This technique is a tool for rapid manufacturing based on organic conducting and semiconducting inks. Inkjet printers can be used as printing device. A key parameter of ink is the ability to generate droplets. Viscosity, surface tension, density, and nozzle diameter, influence the spreading of the resulting liquid drops.

Figure 2-13 shows a printed TFT on Si/SiO_2 [63]. Fabrication of all Graphene TFT also is reported by ink printing method and is shown in Figure 2-14 [64].

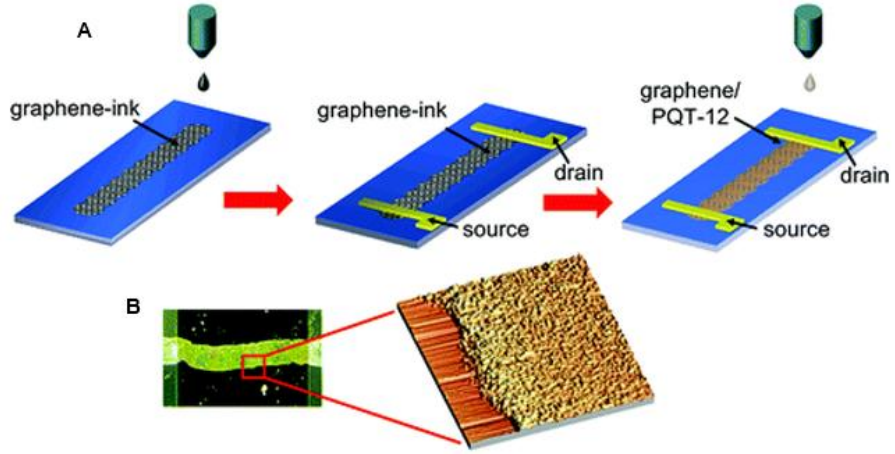

Figure 2-13. A printed TFT on glass substrate with Cr–Au pads as source and drain contacts. A layer of PQT-12 polymer is printed on top (A). AFM images of surface (B) [63]. Reprinted with permission.

Using stamp to transfer Graphene is another technique to make Graphene pattern on desired substrate. The method, named Graphene-on-Demand by Cut-and-choose Transfer-printing (DCT), this method is not suitable to put high-quality Graphene on a large substrate but rather on a specific device active-area often in a size of tenths of micrometers.

The DCT stamps can have pillars with various designs. Pillar arrays are made out of silicon with a thin oxide. Photolithography followed with inductively coupled plasma etching is used to fabricate the pillars. Before transferring the exfoliated Graphene to the substrate the substrate is covered with a fixing layer to ensure fine adhesion between the substrate and the Graphene after stamping (Figure 2-14).

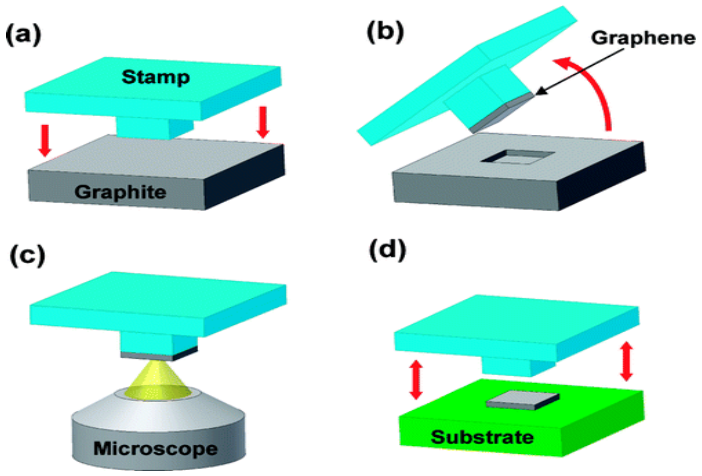

Figure 2-14. DCT Method. (a) stamp with protrusions into the graphite substrate; (b) the stamp cuts and attaches a piece of Graphene using its protrusion edge, and then the separation of the stamp from the graphite (c) quality of the Graphene sheet is checked (d) if the Graphene is good, transfer the Graphene sheet onto the device active-area of another substrate [64]. Reprinted with permission.

Transfer of CVD grown Graphene on copper surface by a cost-effective and lithography-free is shown in Figure 2-15. The Graphene is grown on copper wires which are etched away followed by transfer printing to desired surface using a PDMS stamp. The copper wires can be arranged on PDMS so the transferred pattern design can be determined [66].

2.6.2. Laser Scribing and Patterning of Graphene

Ease of fabrication and high accuracy for future generation of devices such as sensors, radio frequency Identification (RFIDs), organic thin film transistor (OTFT), etc. is of great importance, especially if such devices are flexible and conformable. One fabrication methods is laser scribing of thin films.

This particular method is very suitable for scribing a wide range of materials like polymers, metals, ceramics and glass [67]. Fine features such as patterns for sensors and circuit designs for microelectronics can easily be imprinted [68].

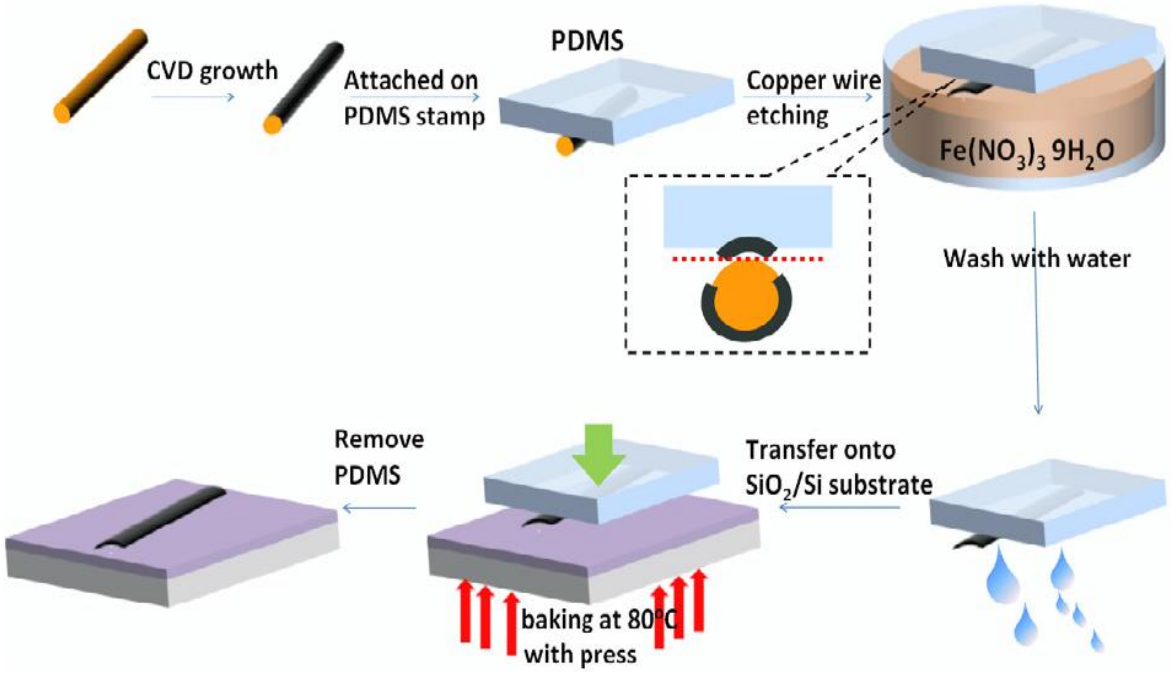

Figure 2-15. Transfer of CVD Graphene strips with a PDMS stamp [66]. Reprinted with permission.

Photo-thermal scribing by laser does not rely on the use of chemicals or high temperatures and shortens the reaction time from several hours to a few minutes or seconds.

In this method laser beam moves on a predesigned pattern and meanwhile scribes and reduces the thin layer surface. Simple, one step reduction of GO has been carried out using flash reduction and 790 nm femtosecond laser. Although films produced by these processes have increased conductivity [18].

One application of laser is fabrication of super-capacitor [67]. Laser beam reduces and patterns graphite oxide films. The ability to reduce and pattern hydrated GO films using laser irradiation has enabled the development of a scalable process to write micro-super capacitors on these films, which work with or without the use of external electrolytes [67].

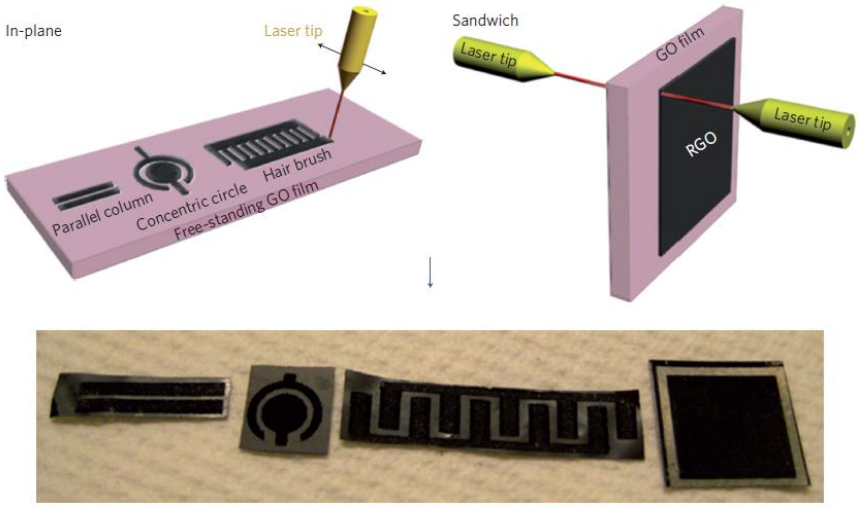

Figure 2-16. Using laser to scribe GO films to fabricate r-GO/GO/r-GO devices with in-plane and sandwich geometries [67]. Reprinted with permission.

In this case trapped water in the graphite oxide layers makes it a good conductor and an electrical insulator at the same time, allowing it to serve as both an electrolyte and an electrode separator. Figure 2-16 shows a sandwich structure of r-GO/GO/r-GO patterns to build electrical double-layer capacitors (EDLC) or super capacitors [67].

Scribing of GO film with pulsed laser is a single step and low temperature technique. The conductive layers of reduced GO with a sheet resistance down to ~700 Ω/☐, are observed. Increasing the number of pulses increases the percent of reduction and reducing sheet resistance. Figure 2-17 compares sheet resistance vs. number of pulses. The majority of oxygen-containing functional groups of GO are removed by the pulsed laser irradiation and enhances electrical conductivity [67] , [68].

Digital video disk (DVD) burner also can be used as a source of laser for writing on a thin film GO. By controlling the pattering times, the resistance of the Graphene can be tuned. This method allows fabricating miniaturized electronic devices. A hundred or more micro super- capacitors can be scribed on a disc in less than half an hour. Figure 2-18 shows the laser scribing of GO film using a DVD writer [69].

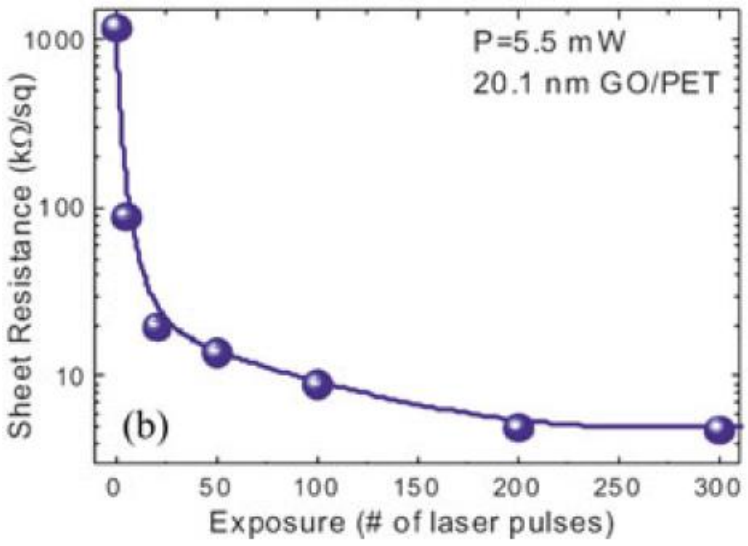

Figure 2-17. Sheet resistance as function of number of laser pulses [68]. Reprinted with permission.

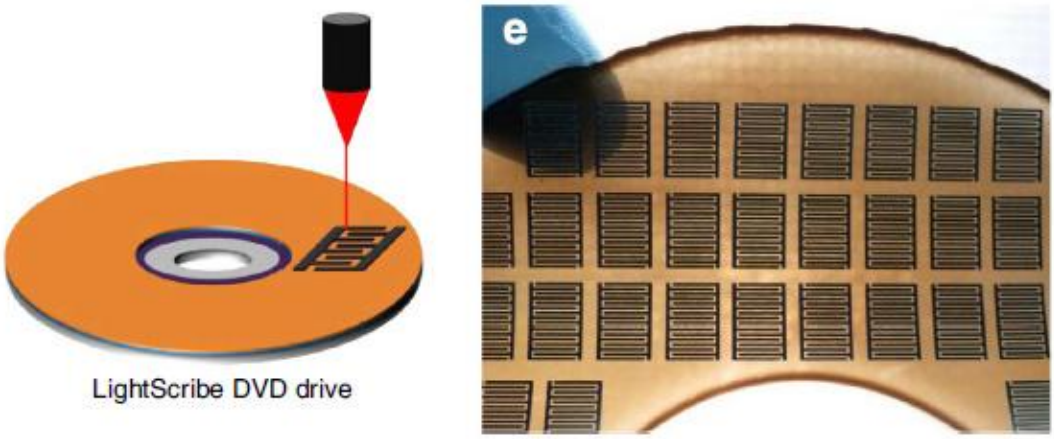

Figure 2-18 . DVD writer to fabricate laser scribed Graphene micro super-capacitor [69]. Reprinted with permission.

2.7. Applications of Graphene

2.7.1. Electronic and Optoelectronic Applications

Graphene has a high carrier mobility which is useful as well as low noise, allowing it to be used as the channel in a field-effect transistor. It has been used as the

conducting channel for field effect transistors (FET) with a variety of gate configurations and materials. Fabrication of all-Graphene planar FET with side gates is reported. The top-gated FET fabrication is reported in several works [70], [71] . Graphene can be used in high frequency field effect transistor but still not as good as technologies such as compound semiconductors (III–V) materials [72].

Others believe that it is unlikely that Graphene makes it into high-performance integrated logic circuits within the next decade because of the absence of a bandgap [6].

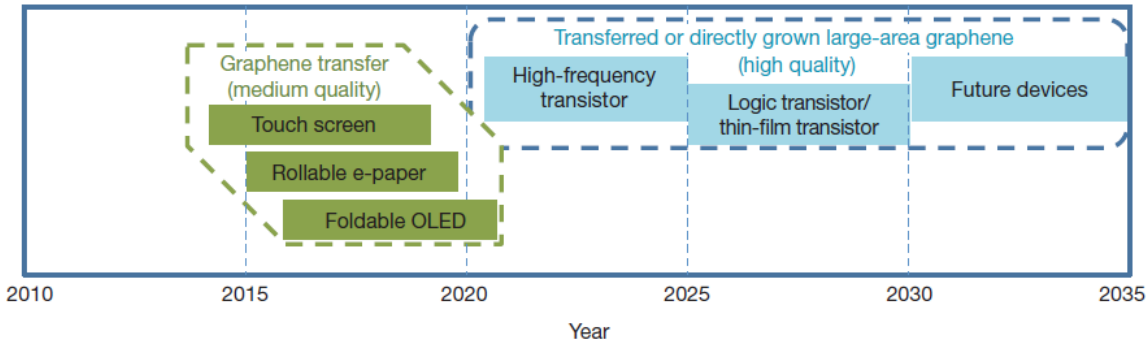

Figure 2-19. Graphene-based display and electronic devices. Possible application timeline [4]. Reprinted with permission.

Excellent electrical conductivity and high transparency are requirements for transparent conductive coatings which are widely used in touch screen, liquid crystal displays, organic photovoltaic cells, organic light-emitting diodes (OLEDs), and organic photovoltaic cells. Graphene meets the electrical and optical requirements (sheet resistance reaching 30Ω per square of 2D area in highly doped samples) and an excellent transmittance of 97.7% per layer [4].

Transparent conductive coating can be made in different qualities, by different preparation methods, so the electors can come in different sheet resistance from 50-300Ω/□. Graphene's unique mechanical properties make it a perfect choice for touch panels. With higher fracture strain it can also be used in bendable devices.

Roll-to-roll production of transparent electrode is reported. Graphene is grown by chemical vapour deposition on copper substrates [73]. Other techniques such as solution-processed Graphene thin films also can apply to fabricate transparent

conductive anodes for organic photovoltaic cells. In this method Graphene electrodes are deposited on substrates by spin coating of an aqueous Graphene, followed by a reduction process to reduce the sheet resistance [74]. Graphene-based paints can be used for conductive ink. One application is electrodes for solid-state dye-sensitized solar cells. These Graphene films are fabricated from exfoliated graphite oxide, followed by thermal reduction [75].

2.7.2. Thin Film Sensors: Pressure and Temperature Sensors

Two dimensional structure of Graphene has properties that are extremely sensitive to the environment. So considering it for sensor applications is quite reasonable. Graphene is very sensitive to various stimuli, such as thermal, mechanical and chemical. So Graphene based sensors may have a lot of potential applications, although the sensitivity of them must meet the practical standard. Recently there are many R&D demonstrations related to Graphene-based sensors.

One of the major research topics in the field of flexible and conformable electronics is electronic skin (e-skin). These sensors usually consist of flexible substrate and circuit with sensors that can respond to physical, chemical or mechanical stimuli. This type of e-skins should be conformable and flexible as their name suggests. A very basic role of skin is to detect mechanical and thermal stimuli so a fundamental component of e-skin would be pressure sensor.

Piezo-resistive sensors transduce the applied pressure on the sensor to resistance output signal. Piezo resistive sensors based on Graphene has been reported. Graphene–polyurethane sponge based pressure sensor is piezo resistive type pressure sensor [76]. This type of sponges shows repeatability and long cycling life as well as capacity of large-scale fabrication. It is believed that fracture microstructure of conductive sponges can greatly enhances the pressure sensitivity to the value achieved by complicated micro or nano manufacture [76].

Fabrication of a field effect transistor (FET) based pressure sensor for e-skin application is reported. This kind of sensor uses CVD grown Graphene and shows 80%

transparency, use of Graphene in the electrodes and semiconducting channels has simplified the device fabrication process [77].

Computer simulation of Graphene-based pressure sensor using conjugate gradient method has been implemented using massively parallel simulator (LAMMPS) code. It has been done on a model of a circular Graphene nano-flake sealing a cylindrical well. The suspended Graphene nano-flake stretches by the applied load. When the applied load reaches a critical value, the Graphene sensor failed. Two type of mechanical failure have been proposed. First a complete detachment of the Graphene flake from the supporting substrate. Second, fracture of atomic bonds within the Graphene flake [78]. Figure 2-20 shows the concept model for this kind of simulations.

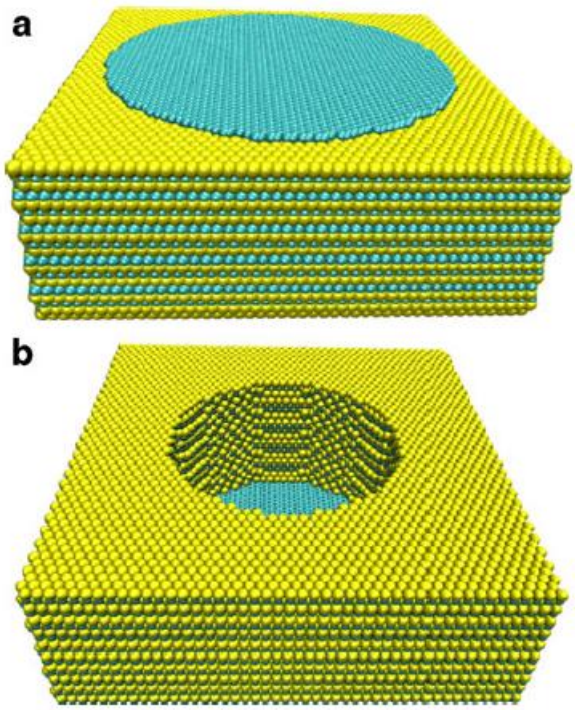

Figure 2-20. Silicone substrate with a cylindrical well covered by a Graphene nano-flake. Blue is Graphene atoms and yellow is silicon atoms (a) Top view. (b) Bottom view [78]. Reprinted with permission.

Very few reports are available for Graphene-based temperature sensor. In one method, Graphene hot wire is fabricated using micro/nanofabrication techniques and the

Graphene films is patterned through electronic beam lithography (EBL) technique. The sensing behaviour of the device is studied by monitoring the resistance change of Graphene as the function of temperature change from room temperature to 80ºC. Results show that Graphene has negative temperature coefficient which means resistances increases as temperature decreases [79]. The negative temperature coefficient of Graphene around ambient temperature (-30 – 40)°C has been confirmed in other works as well [80], [81].

Flexible temperature sensor which is a composite of PDMS and Graphite shows good flexibility and robustness. This types of composite shows the best performance when 15% graphite powder is added. Polymer mixed with conductive fillers shows resistance change as a function of temperature change [82].

Chapter 3

Fabrication of Graphene-Based Sensor

3.1. Introduction

In this chapter, fabrication of Graphene-based sensors is explained. Several steps needed to fabricate a functional sensor such as substrate preparation, micro contact printing of conductive path, drop casting or spraying of Graphene, proper reduction of Graphene utilizing laser, as well as making electrodes and making connection between conductor and sensing parts and thermal curing of thin film and metal ink. Also all steps are important but the most important step is reduction of Graphene by laser.

In chemistry, removal of oxygen atoms from a structure is called “reduction”. The exact definition of a reduction reaction is the gain of electrons or a decrease in oxidation state by a molecule, atom, or ion. For example: the reduction of nitrate to nitrogen in the presence of an acid can be shown using (Eq.**(3**)):

$$2\ NO_3^- + 10\ e^- + 12\ H^+ \rightarrow N_2 + 6\ H_2O \qquad (3)$$

In this example Nitrate (NO_3) loses its oxygen atom (or gains electrons) and reduces to Nitrogen (N_2). The same can be done to reduce GO. Figure 3-1 shows the structure of GO and r-GO [83]. Several different ways for reduction of GO has been proposed. Main approaches are chemical and thermal reduction. Chemical and solution based reduction is discussed in chapter 2. The preferred method is laser reduction of Graphene. Using laser as a reduction tool is a very fast, simple, chemical-free, room temperature process that employs the photo thermal reactivity of GO. This process can be applied on thin film Graphene deposited on variety of substrates and by changing the laser parameters the electrical properties of thin film Graphene can be tuned to some

degree. Reduction of Graphene oxide can be evaluated by measuring resistance changes. Removing more oxygen makes the structure more conductive.

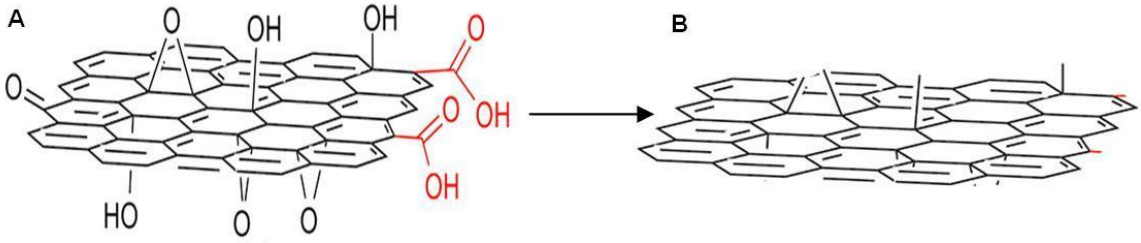

Figure 3-1. Structure of GO (A) and r-GO (B) [83]. Reprinted with permission.

3.2. Overview of Sensor design

A sensor is a device that detects changes in quantities of certain parameters and provides a corresponding output, generally as an electrical, mechanical or optical signal; for example, a thermocouple is a temperature-measuring device consisting of two dissimilar conductors that contact each other at one or more spots. A thermocouple produces a voltage when the temperature of one of the spots differs from the reference temperature at other parts of the circuit [84].

Graphene oxide (GO), is of moderate electrical performance when compared to Graphene, mainly due to the presence of oxygen related defects in the Graphene lattice. Reduction of Graphene oxide is common method to increase the electrical properties of Graphene. The efficiency of reduction strongly varies on the method and process parameters but residual oxygen groups and defects are commonly observed [85].

3.2.1. Flexible Temperature Sensor Design

Temperature is the most widely measured environmental, industrial… variable. Measurement of real time temperature data is vital in oil and gas, food, cosmetic… industries. For example in Pharmaceutical industry, inaccurate temperature measurement might ruin a batch of product worth hundreds of thousands of dollars. For this reason, each measurement system needs to be evaluated and carefully engineered to satisfy the requirements of the process [86]. Measurements are typically made using a

sensor (usually a thermocouple or an RTD) and a signal conditioning circuit to amplify the sensor's low level (ohm or mV) signal to a more robust current signal.

A thermocouple consists of two wires of dissimilar metals joined at both ends. A voltage is created when the temperature applied to one end or junction differs from the other end. This phenomenon is known as the *Seebeck* effect, which is the basis for thermocouple temperature measurements. RTDs are based on the principle that electrical resistance of a metal increases as temperature increases. Thus, a temperature measurement can be inferred by measuring the resistance of the RTD element [86].

RTD's are characterized by their Temperature Coefficient of Resistance (TCR) also referred to as its alpha value. Temperature Coefficient is relative change of a physical property that is associated with a given change in temperature. Each resistance versus temperature relation for an RTD is qualified by a term known as "alpha". Alpha is the slope of the resistance between 0°C and 100°C. This is also referred to as the temperature coefficient of resistance (Eq. (4). Platinum is the most common material in industrial RTD with α=0.00385°K^{-1}. (British Standards Association,B.S. 1904-1964)

$$R(T) = R(T_0) \times (1 + \alpha \Delta T) \qquad (4)$$

Figure 3-2 shows a schematic of Industrial RTD Sensor. Fabrication of such sensor (based on Platinum) has following steps [86]:

- Depositing a thin film of pure platinum on a ceramic substrate in a maze-like pattern (This pattern acts as a long, flat, skinny conductor, which provides the electrical resistance)
- Stabilization by a high temperature annealing process
- Sensors encapsulated with a thin glassy material

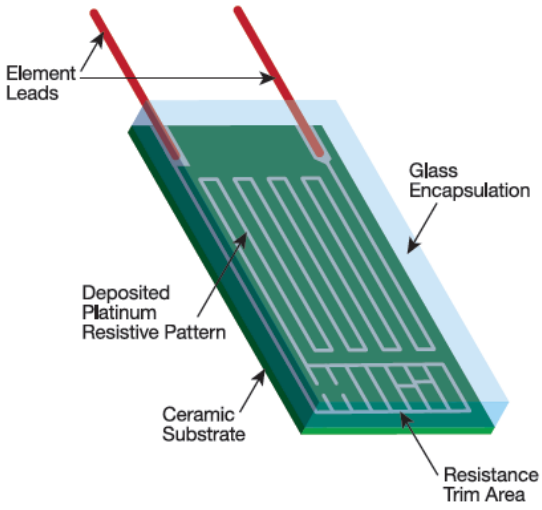

Figure 3-2.Scheme of thin film RTD [86]. Reprinted with permission.

In order to use Graphene as thermistor we need Graphene to be patterned to have a long maze like or other convenient shape. The resistance of platinum is low so usually patterns are designed with relatively high length-to-width ratio in order to achieve a high resistance and a uniform temperature distribution. The design of the Graphene thermistor can be tuned to achieve the desired value of resistance. In order to do this we need to know the resistance of a specific length of Graphene and then decide the total length. Design should be small to lower the cost of manufacturing. It should be small enough in order to have several sensors in a small space. It should have enough length to achieve the desired resistance to be detected. And small enough to be independent of mechanical bending effect on resistivity.

Many papers have been published regarding the design of micro size temperature sensor using lithography and RIE [87], [88], [89] mostly using Au as sensitive material. As mentioned before all sensors based on metal as sensor materials come with a relatively high length-to-width ratio. Some of common sensor patterns are similar to Figure 3-3.

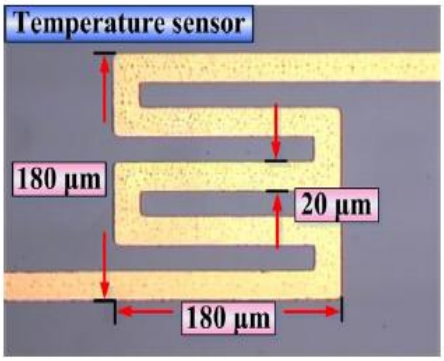

Figure 3-3.A typical Temperature sensor pattern [87]. Reprinted with permission.

Fabrication of such small features needs photo lithography methods, micro contact printing, etching, EBL, stamping…. Design and Fabrication of a Graphene thermistor has been reported using mechanically exfoliated bilayer Graphene films and patterning by EBL technique. The highest resistance change with temperature has been seen in the bilayer Graphene comparing to monolayer and few-layer as the temperature elevated from room temperature to 80^0C [79].

A small feature can't be patterned using high power laser (lase cutter machine) scribing and the pattern width is much larger than 20 µm on Graphene. Laser scribing of Graphene is not 100% perfect so the quality of r-GO is not representing the pure Graphene. The resistance of Graphene over a small path (5 mm) is high enough to detect the effect of temperature of resistance change. Measuring the resistance of scribed Graphene using probe station and AMPROBE 33XR-A multi meter, shows 250Ω for a sample with 5 mm length, and the proposed sensor pattern for Graphene as temperature sensor is shown in Figure 3-4. This design has an array of 8 scribed lines of Graphene (which are 8 sensors) with conductive lines of silver made by stamping of silver nano wire. These 8 sensors can be used to measure the resistivity. The temperature sensor is fabricated in the form of arrays, so comparison of different temperature readings is easy. A typical design for testing the temperature is like Figure 3-4. The conductive patterns are showed as dotted lines and sensing part is outlined in the picture. The fabricated final sensor array is shown in Figure 3-5.

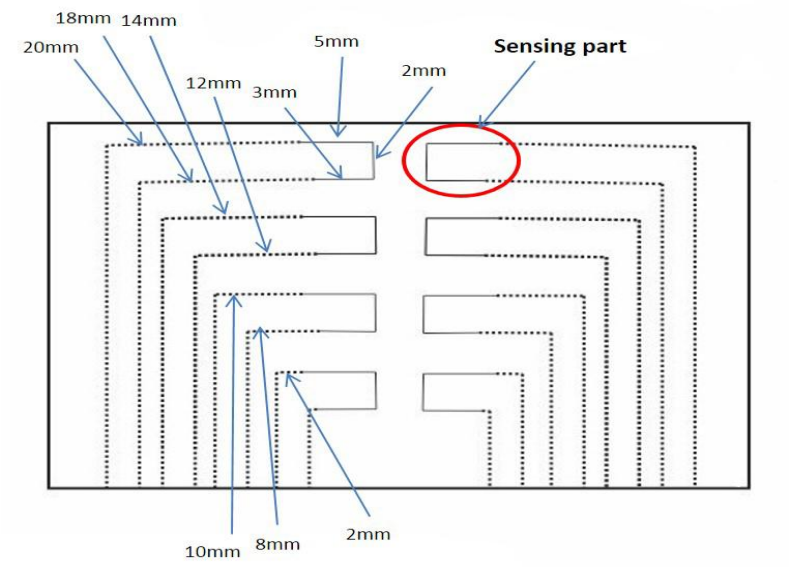

Figure 3-4. Design of temperature sensor with dimensions.

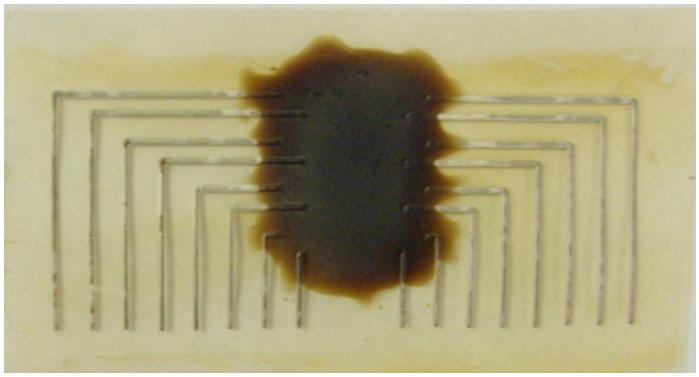

Figure 3-5. Fabricated Graphene-based sensor for temperature measurement.

3.2.2. Flexible touch Sensor Design

Touch sensor is designed to have almost the same area as a fingertip has. So the whole sensing part can be touched by fingertip. It is designed in spiral shape (Figure 3-6). The array pattern is designed using a commercially available software package (Corel Draw® X6).

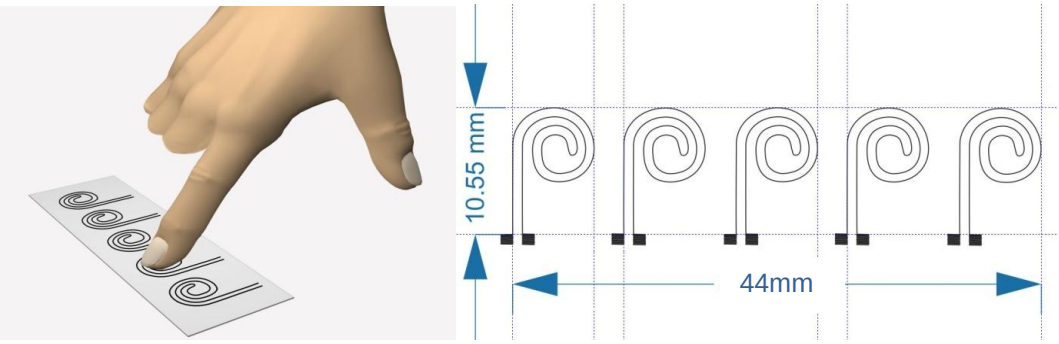

Figure 3-6. Schematic of Graphene touch sensor with dimensions.

3.3. Fabrication of Graphene Sensor

3.3.1. Selection of Substrate

The first step is selection of substrate to fabricate the sensor based on it. The preferred substrate is PET, because it is cheap, flexible, transparent and easy to work with.

Flexible PET substrate is utilized by being cleaned with methanol, distilled water and the left over liquid dried at room temperature. Different PET sample size has been used as substrate to design and fabricate different sensors (Temperature and touch sensor).

- For Temperature sensor array (array of 8 sensors): 6cm x 2cm rectangle
- For Touch sensor array (array of 5 sensors): 4.5 cm x 1 cm rectangle

3.3.2. Preparation of Electrode for Sensors: Silver Nanoparticle and Patterning

In addition to sensing parts, conductive paths are needed too. To make conductive path, stamping method for transferring of silver nano particles (AgNPs) is chosen. Conductive paths in the design have been made of silver nanoparticles (AgNPs). A solution of AgNPs in toluene (5 wt. %) is prepared as silver nano ink. Required AgNPs are synthesized using the recipe from other works with modification [90].

After extraction of AgNPs, the particles are dissolved in toluene to make different weight percent solutions from 5 wt. % to 20 wt. % solution. In order to transfer Nano particles to the PET substrate Micro-contact printing method is employed based on other works [91].

3.3.3. Preparation of Graphene Oxide Thin Film

3.3.3.1. Drop casting of GO solution

Graphene is utilized in the form of GO solution in water (0.5 wt. % GO, Angstron Materials Dayton, OH, USA). This GO solution is very stable and no precipitation observed after one year of purchase. It is drop-casted on PET in specific volumetric amount (from 0.5ml to 2ml depending on substrate area) using a pipet and dried overnight at room temperature.

3.3.3.2. Aero-sol Spray Coating of GO Solution

Besides drop casting, Graphene oxide solution is sprayed using air brush also. This is done to see if the covering of PET is better or not in this case. GO is hydrophobic and PET surface should be functionalized using dopamine solution, Also spraying of GO on PET surface is not an effective way and waste a lot of GO, in fact 50 % of solution is wasted during spraying process so this approach is not effective way of coating. In addition, thickness of coating is very small and is not enough for further scribing by laser. A minimum thickness of thin film on substrate is needed in order to scribe it with laser. Too thin layer cannot be patterned by laser because the layer can be removed even by very low laser energy.

3.3.3.3. Thermal treating of GO Thin Film

In order to remove bonded water and other possible solvents from thin film also to relieve internal stresses and refine the structure; Graphene film is cured in vacuum oven (Mandel OV-11) at -0.09 Mpa and 150°C for 1 hour.

3.4. Laser Scribing of Thin Film

Thin film of GO on PET is scribed by a CO_2 laser (Universal Laser system – VLS 3.6) at specific paths (Figure 3-4 & Figure 3-6) to form the sensing parts. The CO_2 laser (0.6 Watt, 10.6 µm in wavelength, and 200-300 µm in spot size) is irradiated with different laser beam speed, beam power, and beam distance to surface to obtain the optimal results in order to achieve higher conductivity of r-GO.

3.4.1. Optical Microscopy Images

Optical images of after scribing of GO shows some basic information such as width of reduced tracks and the amount of materials removed by laser beam related to beam power or speed. By increasing speed (less exposure of Graphene to the beam) the ablation is less and the remaining Graphene on surface is more and the conductivity increases. Also by increasing the Power the possibility of burning out of materials from surface increases. (Figure 3-7 shows the changes in scribed line by changing the speed of beam). The feature width is around 0.25mm.

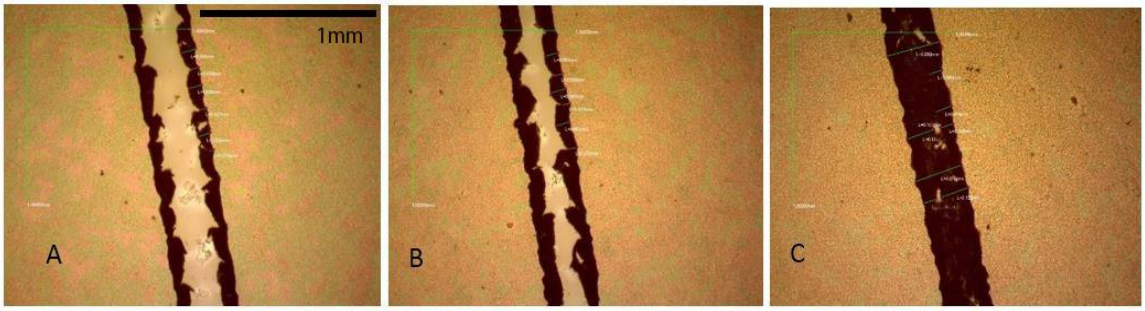

Figure 3-7.Optical microscope images showing the effect of scribing speed and power on GO, P=0.9 watt and S=7.6cm/sec (A), P=0.9 watt and S= 12.5 cm/sec (B), P=0.6 and S=12.5 cm/sec (C).P=power, S=speed.

3.4.2. Speed of Scribing by Laser Beam

Speed of movement of laser head can be adjusted, so the exposure time on substrate may vary depending on speed. The other parameters like power and distance of laser head should be fixed. After the patterning and reduction of GO, the resistivity of r-GO thin film is measured. The measured resistivity depending on speed of scribing is

shown in Figure 3-8. By keeping the power (at minimum which is 0.6 watt) and height (3.4mm) fixed, the minimum resistivity is achieved when the speed is 12-13 cm/sec for this specific laser machine.

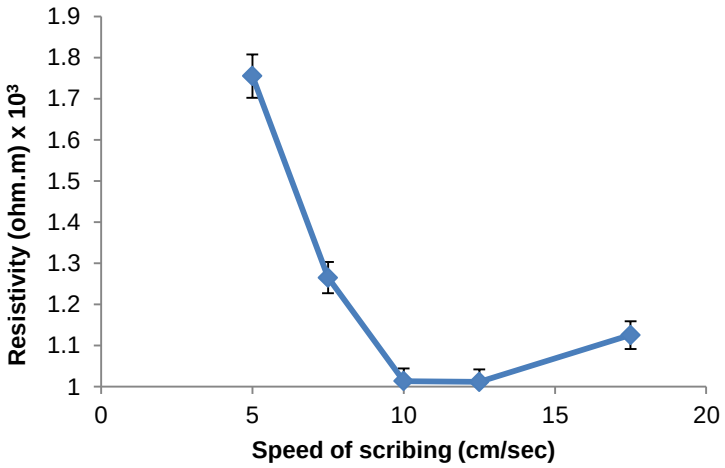

Figure 3-8. Speed of scribing vs resistivity.

3.4.3. Laser Power

The power of laser beam is of extreme importance when it comes to scribing a thin film. High power can burn everything it shines to; too low laser power cannot scribe or reduced the GO at all or in very low amount. Laser powers higher than 3 watt damage the surface and burn off the GO so the scribed line will be non-conductive. Figure 3-9 shows how different laser powers effect the scribing and resistivity of thin layer.

3.4.4. Distance of Laser Head to Surface

Although the laser beam is very narrow and almost parallel but the distance of it from surface is critical. By changing the gap between surface of sample and laser head, the film quality and conductivity of r-GO can change. At a specific distance from laser head, the beam is focused on the film surface i.e. if the sample places out of focus, the GO cannot be reduced efficiently (Figure 3-10 & Figure 3-11). Figure 3-12 shows scribing of film at two different speeds. For each speed, the laser head height is changed

and the measured resistivity is plotted vs. height. For both speeds, the minimum resistance is achieved at 3.4 mm. So this height is selected as the optimum.

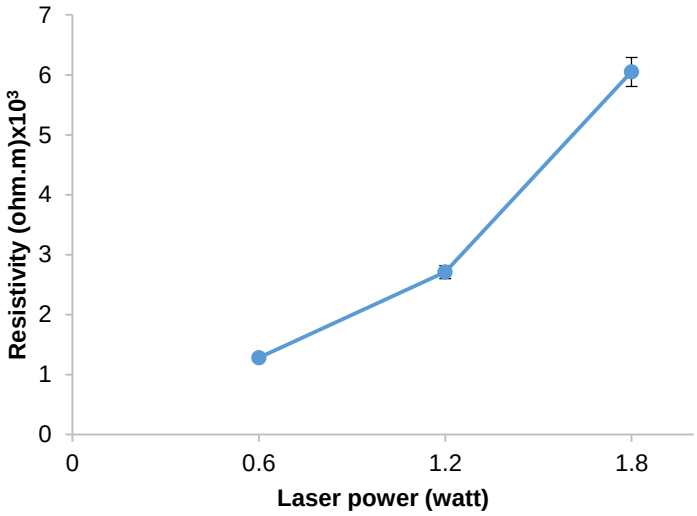

Figure 3-9. Laser beam power vs resistivity.

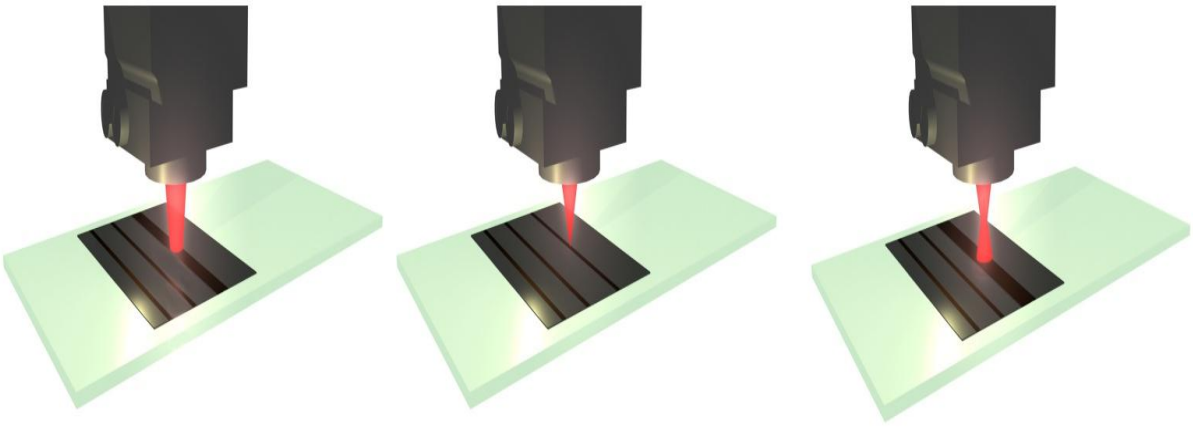

Figure 3-10. Different spot size of laser vs. distance to surface.

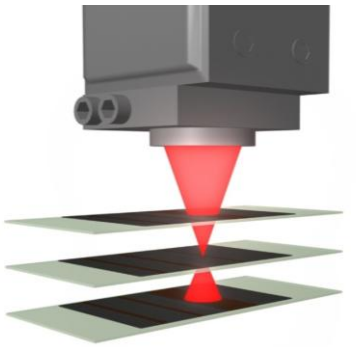

Figure 3-11. Different placement of sample from laser head and focal point.

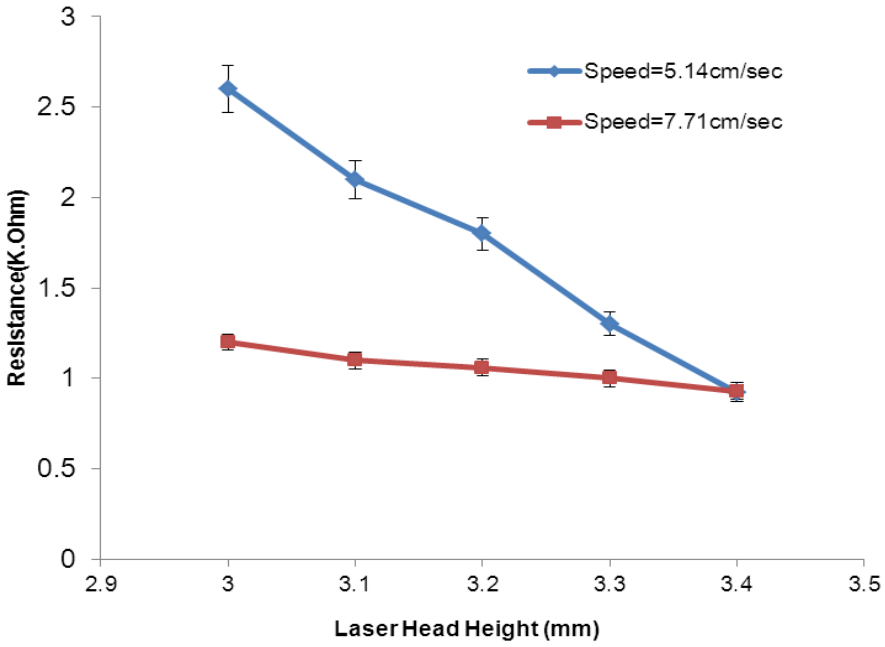

Figure 3-12. Resistance vs. Laser head height.

3.5. Final Assembly and data acquisition

In order to make connection between metal path and sensing part, conductive silver epoxy paste is used; this type of paste has high conductivity and cannot interfere with

sensor behavior. In case of touch sensor, copper wires glued to Graphene with silver paste directly.

Simple circuit converting from resistance to voltage is designed in order to acquire sensor's voltage output. A NI6008 data acquisition kit is wired to the circuit and connected to a pc through USB port. NI max interface is used to visualize data (Figure 4-17D). A digital force gauge (Dillon Model GS) with hand wheel test stand is used to apply exact amount of pressure on sensors from 50 mN up to 500 mN. The applied force is converted to pressure.

3.6. Fabrication of Hybrid Graphene-based Sensor

As an extra step of fabrication of Graphene based sensor, composition of Silver nano wire and Graphene is used to see the effects of using hybrid compounds in fabrication of capacitor. The advantages of Graphene-Metal nano structures have been discussed in chapter two. Silver nano wire is synthesized using recipe from previous works [92]. Figure 3-13 shows SEM images of synthesized nano wires.

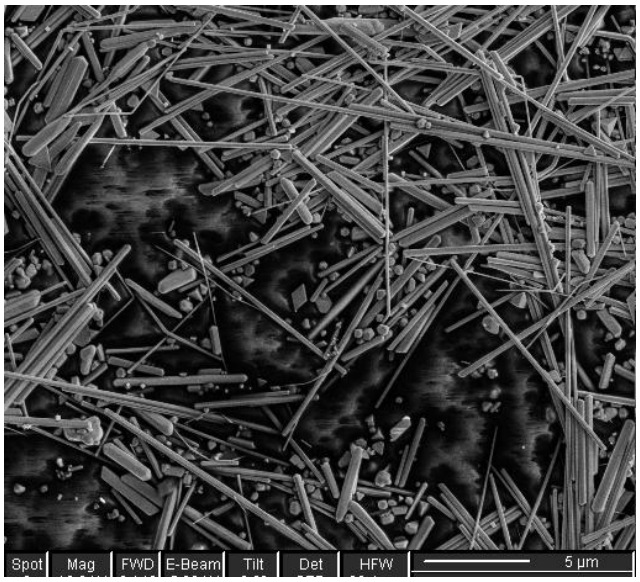

Figure 3-13. SEM images of AgNW.

Isopropyl alcohol (IPA) is used as solvent to prepare silver nano wire solution. 5 samples of AgNW with different weight ratios (1%, 1.5%, 3%, 6%, and 9%) are prepared

by mixing in IPA. Then 1ml of each sample is added to 1ml of GO solution. The final samples are as follows:

- AgNW-GO9 (9% wt. AgNW)
- 2- AgNW-GO6 (6% wt. AgNW)
- 3- AgNW-GO3 (3% wt. AgNW)
- 4- AgNW-GO1.5 (1.5% wt. AgNW)
- 5- AgNW-GO1 (1% wt. AgNW)

The AgNW-GO mixture is drop casted on PET, dried overnight, and drop casted for a second time. Next, sample is cured in vacuum oven at 150°C. Final step is laser scribing of hybrid thin layer to make predesigned capacitor pattern (Figure 4-19). Addition of silver nanowires makes the thin film rougher than only GO so the laser power should be increased to pattern the hybrid surface effectively. Laser parameters for scribing the hybrid layer are; Power: 1.2 watt, speed: 20cm/sec (80% max speed), height = 3.4mm. The capacitance has been measured to see if this type of capacitor can show responsibility to mechanical forces (touching in this case).

Chapter 4

Characterization and Analysis

4.1. Introduction

Laser-induced reduction is a very fast, facile, chemical-free, room temperature process that exploits the photo thermal reactivity of GO. Since the process can be applied to GO thin films deposited on plastic substrates, the electrical and chemical properties of r-GO-based devices can be controllably altered in situ. In this chapter chemical, electrical and morphological changes of GO, after scribing by a laser beam is presented and discussed. Figure 4-1 shows the reduction mechanism. It shows removal of oxygen groups and how laser beam heat up the surface of GO and removes oxygen atoms as well as moisture and bonded water.

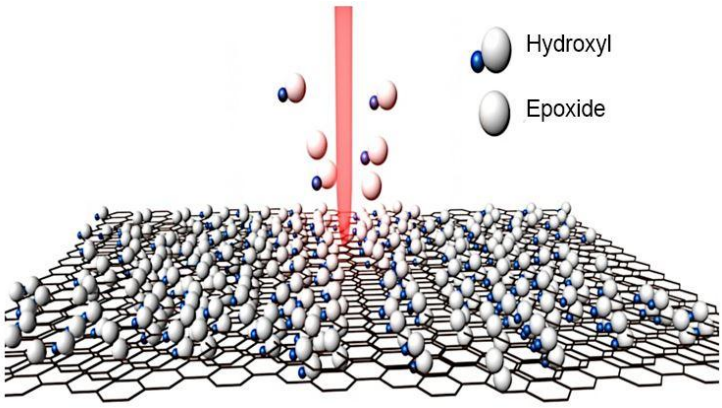

Figure 4-1. Schematics of Photo-thermal reduction of r-GO.

In general the mechanism of ablation depends on:

- Quality of film and coating (thickness, cleanness, homogenous surface).
- Properties of the material being ablated.

- CO_2 laser parameters such as laser beam speed, laser beam power, laser head distance, wavelength of radiation (10.6μm in this case).

4.2. Characterization of r-GO Thin Film

4.2.1. FT-IR Characterisation

Fourier transform infrared spectroscopy (FTIR) is a technique which is used to obtain an infrared spectrum of absorption, emission, photoconductivity or Raman scattering of a solid, liquid or gas. This technique is employed to see if the carbon-oxygen bonds dissipated after scribing or not. Exposure to the laser beam removes components such as oxygen and hydrogen bonds from the surface and changes the GO to conductive r-GO. Photo-thermal removal of the oxygen groups of the GO, mainly from hydroxyl and alkoxy, takes place during laser scribing of the GO film. It has been demonstrated that the carbon content bonded to oxygen is reduced by laser scribing, indicating that the majority of oxygen groups are removed and effective reduction takes place [93]. Figure 4-2 shows the intensities of the FT-IR peaks corresponds to the oxygen functionality groups such as C=O at 1726 cm^{-1}, peaks of O–H groups at 3395 cm^{-1}, the C–O (alkoxy) stretching peak at 1052 cm^{-1} have decreased drastically. These observations confirms that most oxygen functionalities in the GO have been removed [94], [95]. Laser induced reduction of GO in N_2 environment enhances the quality of r-GO by the removal of more oxygen groups during laser irradiation [18].

4.2.2. EDX of GO and r-GO

Energy-dispersive X-ray spectroscopy is used in order to identify the elements presented in thin film. EDX is done using “FEI, Model Dual beam 235”. The EDX results for GO and r-GO are shown in Figure 4-3. Looking at the oxygen content of samples before and after scribing of GO, It can be seen that oxygen atoms are reduced to a forth. This observation is in agreement with FT-IR graphs which show that the peaks of “alkoxy” group decreased drastically. So chemical reduction of GO into r-GO is obvious from the analysis.

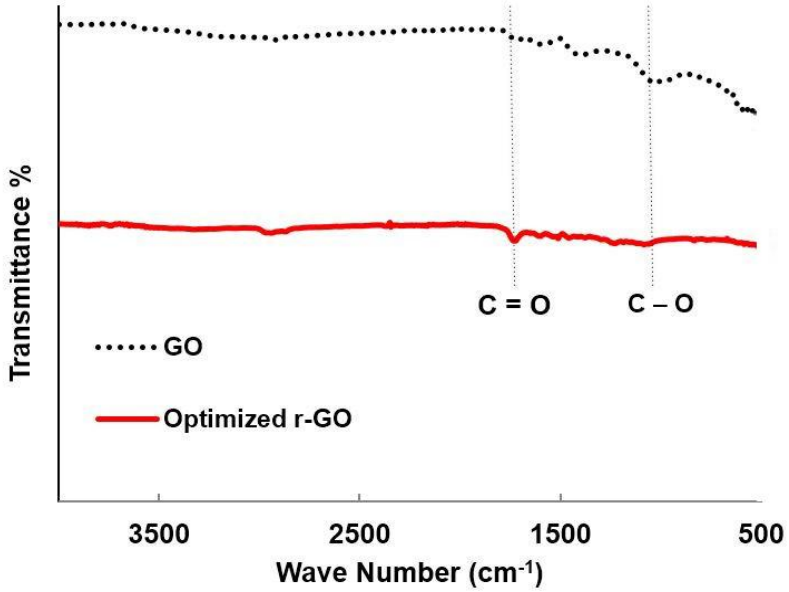

Figure 4-2. FTIR Graphs of GO and r-GO.

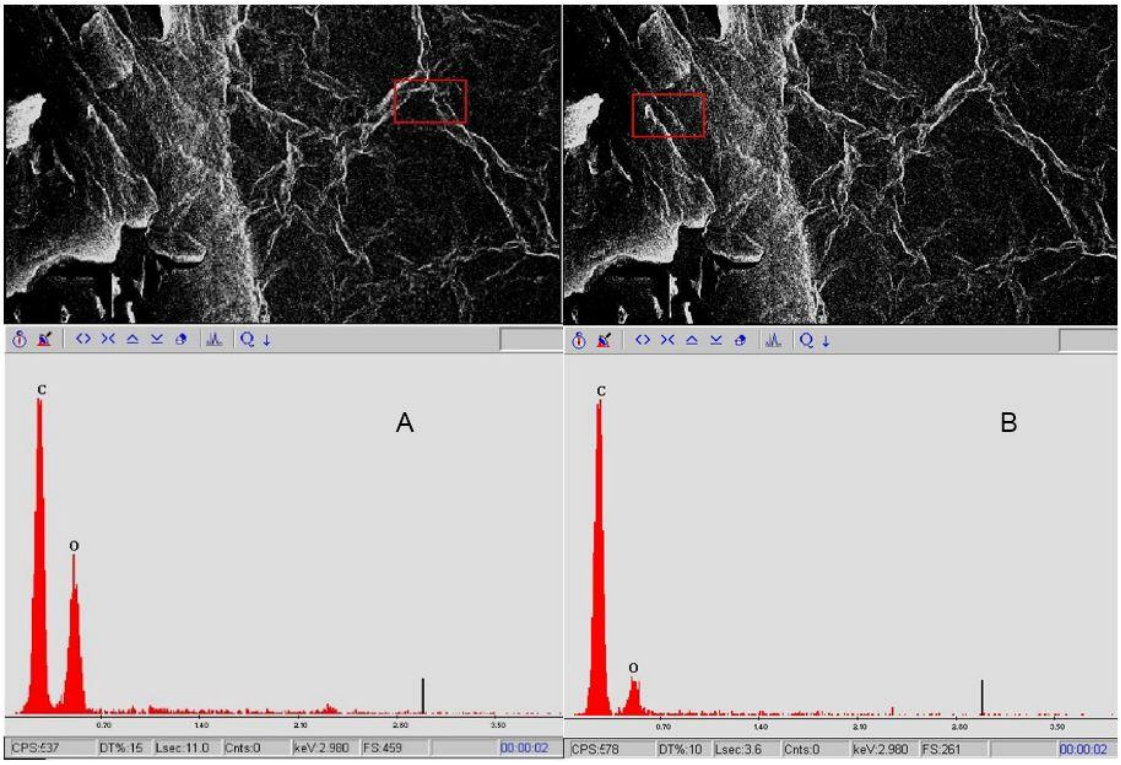

Figure 4-3. EDX Comparison of GO (A) and r-GO (B).

4.2.3. Confirmation of Reduction (Electrical properties)

As mentioned in Chapter 3, different laser parameters need to be selected carefully to get a high quality final product. Scribed GO shows totally different electrical properties than un-scribed GO. Figure 4-4 shows plot of these data for more convenience. Table 4-1 contains the measured value of resistance as a function of different laser head from the surface for two different laser speeds.

Table 4-1. Value of resistances as function of laser head distance from surface

	Resistivity (Ωm)	
Beam distance	**Speed (12.85cm/sec)**	**Speed (18cm/sec)**
3	4.30E-04	6.55E-04
3.2	4.35E-04	7.34E-04
3.4	3.96E-04	4.62E-04
3.6	4.08E-04	7.31E-04
3.8	3.98E-04	7.16E-04

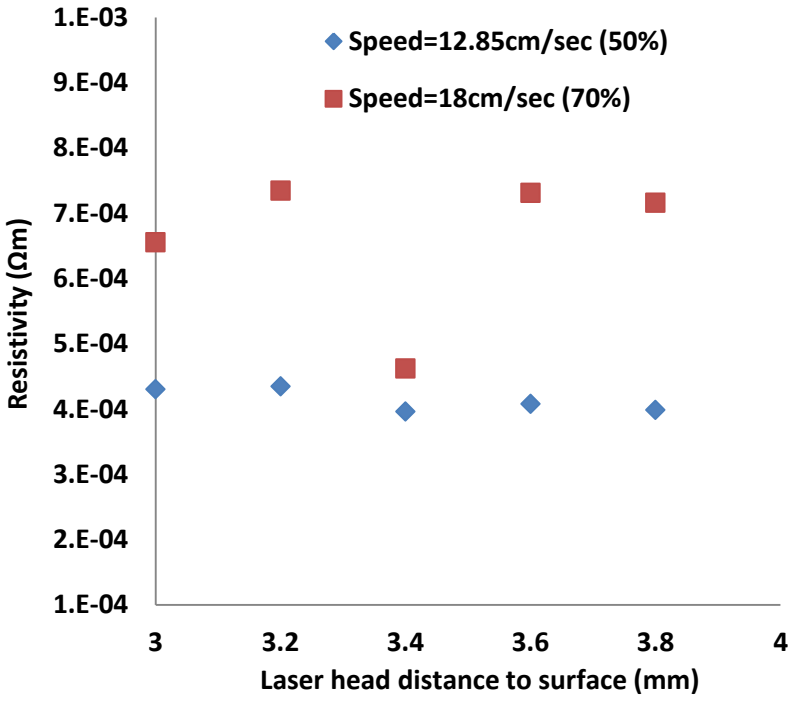

Figure 4-4. Laser head distance vs. resistivity in two different scribing speeds.

4.2.4. Morphology Characterization

4.2.4.1 Optical Microscope

Figure 4-5 shows the morphology of GO thin film before and after scribing. The roughness of surface dramatically changes after scribing, it can be attributed to removal of oxygen and destructing of structure as well as thermal expansion of GO. Release of gases can displace GO layer and make channels and gaps.

4.2.4.2 Atomic Force Microscopy (AFM) of r-GO Surface

AFM imaging is a common method for studying morphology of thin films. Running AFM on scribed GO is very difficult because of high surface roughness. AFM is very sensitive on surface roughness.

Figure 4-6 compares before and after scribing images of GO and r-GO. AFM Imaging shows that, the thickness of sample increases 3-4 times after scribing from 3.5 µm to 16 µm. As discussed before the displacement of Graphene layers and release of gas made gaps and slits on the surface. These changes suggest that the surface morphology altered from smoother to a much rougher surface by damaging the GO layer into r-GO which confirms the SEM results in next section. Oxygen atoms are bonded to top and bottom layer of Graphene and after scribing and removal of oxygen those layers separated and displaced from a flat form to a random orientation.

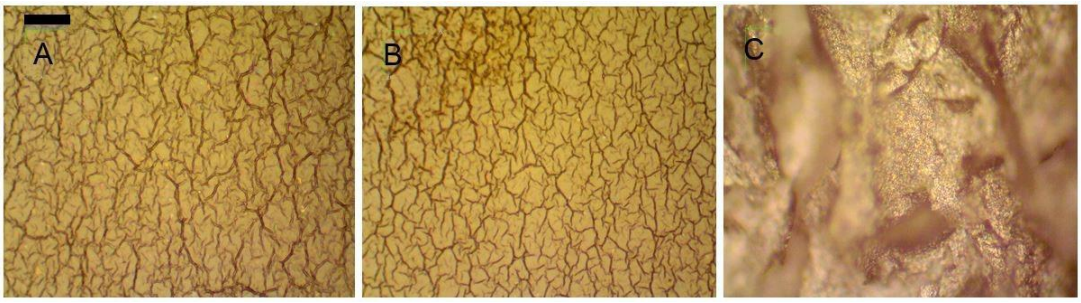

Figure 4-5. Optical images of GO (A) thermally cured GO (B) and r-GO. Black bar scale is equal to 25 µm.

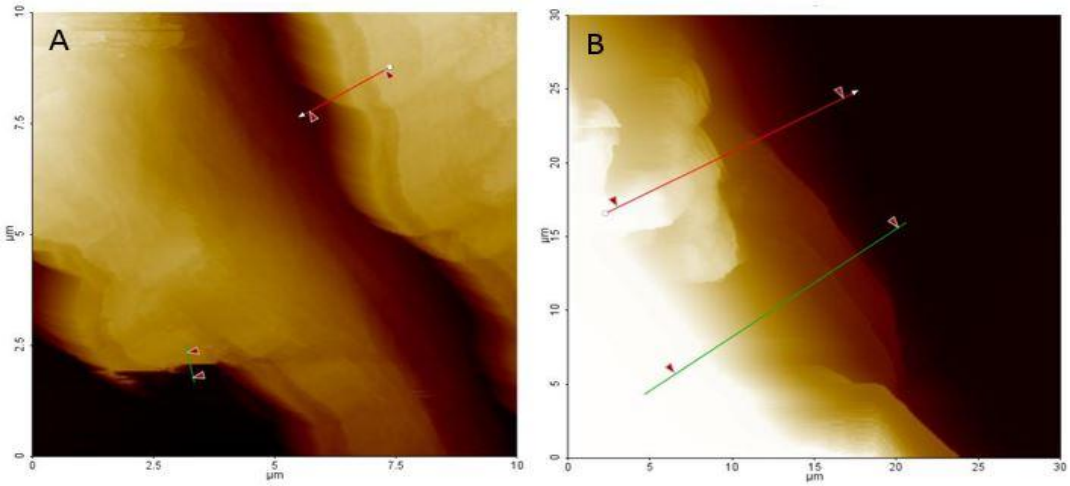

Figure 4-6. AFM images of GO (A) and r-GO (B).

4.2.3.3. SEM of r-GO Surface

Figure 4-7 shows SEM image of GO and r-GO with high contrast. The morphology of GO surface is totally different from scribed area and visually it is very rough that is in agreement with optical microscopy images. Similar results of morphology and surface change has been reported elsewhere [67], [95], [82].

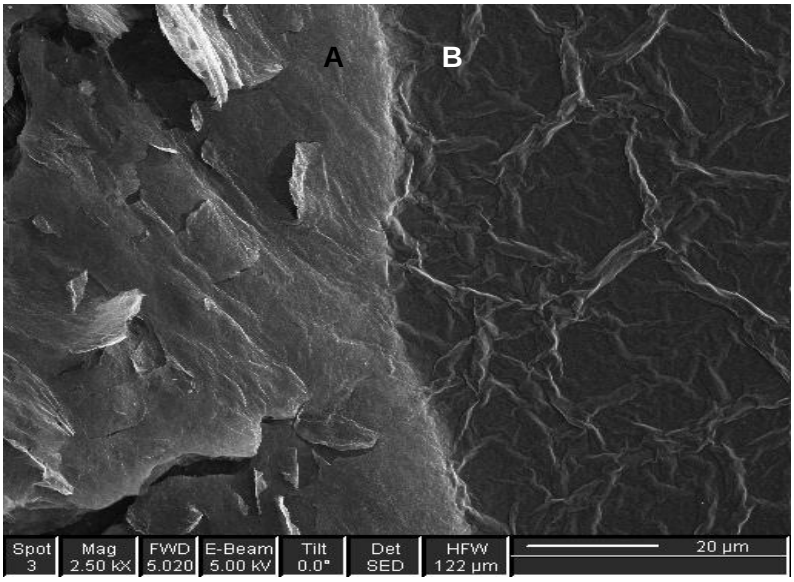

Figure 4-7.SEM Images of r-GO (A) and GO (B).

4.3. Hybrid Graphene Capacitor

Hybrid thin film of AgNW-GO is made to see how addition of AgNWs changes the properties of Graphene-based thin films especially in terms of electrical properties. The composition and fabrication steps of hybrid thin layer are described in chapter 3. In this section electrical and morphological behaviour of hybrid film is presented. Hybrid composition of thin layers is a mixtures of GO and AgNW with different weight ratio. Effect of AgNW concentration is analyzed using imaging techniques along with electrical properties measurement.

4.3.1. Measurement of Electrical properties

Resistance data for hybrid film is presented in Table 4-2. The resistance per millimetre is measured using multi meter and also probe station with probes one millimetre apart. The AgNW percentages in hybrid samples are 1, 1.5, 3, 6, 9 %. The trend shows that increasing the content of AgNW decreases the resistance of sample. As AgNW has higher conductivity than r-GO, it is anticipated that the role of AgNW is increasing the conductivity. From the table, sample with 9% AgNW, shows minimum resistance among 5 different samples although the resistance is not decreased drastically. Increase of AgNWs percentage increases the contact resistance so the trend is not exactly proportional to amount of AgNWs.

Table 4-2. Electrical properties of Hybrid AgNW-GO (After scribing)

Sample (Percentage of AgNW)	1%	1.5%	3%	6%	9%
Resistance (per mm)	1.85kΩ	0.8kΩ	0.7kΩ	0.65kΩ	0.44kΩ

4.3.2. Morphology of Hybrid Film: Optical Microscope, AFM, SEM

Morphology of hybrid film has been investigated by variety of imaging techniques, before and after scribing, for 5 different composition of AgNW-GO. Similar to only Graphene samples, these hybrid samples show rough surfaces after scribing. Figure 4-8 and Figure 4-9 show that thermal curing makes the surface of films smoother to some degree and comparing the before and after curing images confirms this statement. It is more obvious in case of lower percentage of AgNW, although for higher

percentage AgNW (9%) or AgNW (6%) a high density of wires are on the surface and lead to a rough surface. Figure 4-10 shows AFM images of hybrid samples for 1-1.5%, Scan size is 40µm x 40µm. 3D images are in agreement with optical images and confirm that the roughness decreases after thermal curing mostly because of removal of stress of surface and thermal expansion and displacement of wires. By increasing the content of AgNW (Figure 4-11), thermal curing does not show considerable effect on surface and no more reduction on surface bumps. There are a lot of metal wires on surface and thermal expansion of GO layer is not enough to cover the wires.

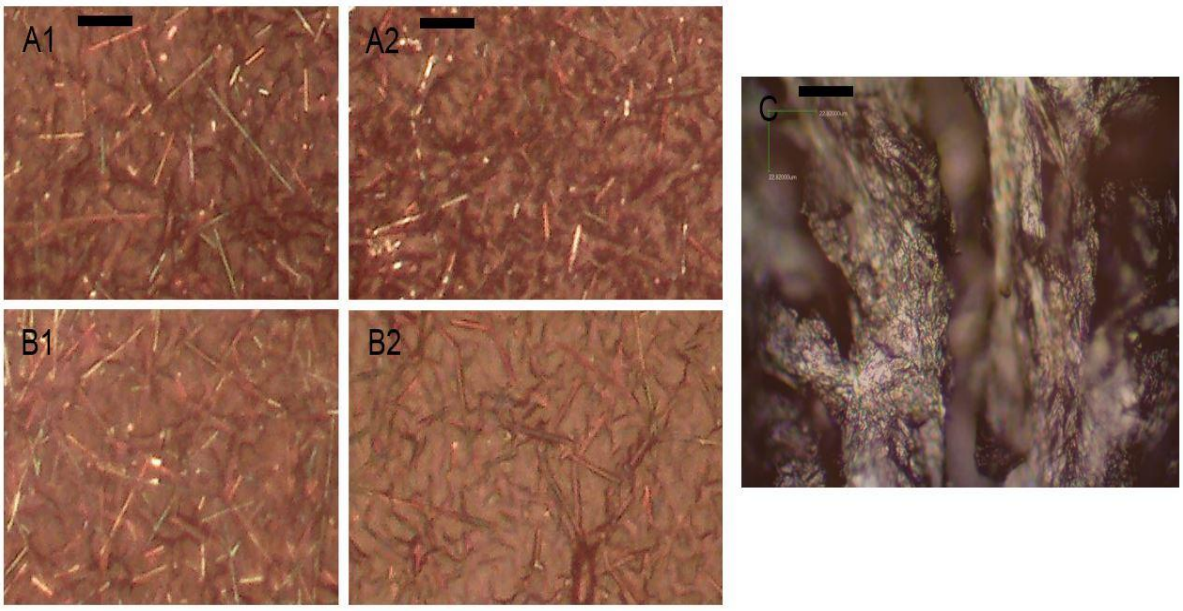

Figure 4-8. Optical images of 1% AgNW before thermal curing (A1), after thermal curing (A2), 1.5% AgNW before thermal curing (B1) after thermal Curing (B2), after scribing (C).Black bar scale is 30µm.

Figure 4-12 Compares AFM images for 3 different samples (3%, 6% and 9%) before and after scribing. At first it looks like that scribing of hybrid samples removed AgNW from them and the surfaces are very smooth, the disappearance of AgNW can be explained by considering the thermal expansion and layered structure of r-GO. Displacement of Graphene layer covered the AgNWs beneath. From Figure 4-12, the silver nano-wires cannot be seen and it looks all AgNWs are removed. Scanning electron microscopy can be employed to investigate the surface of thin film more accurately.

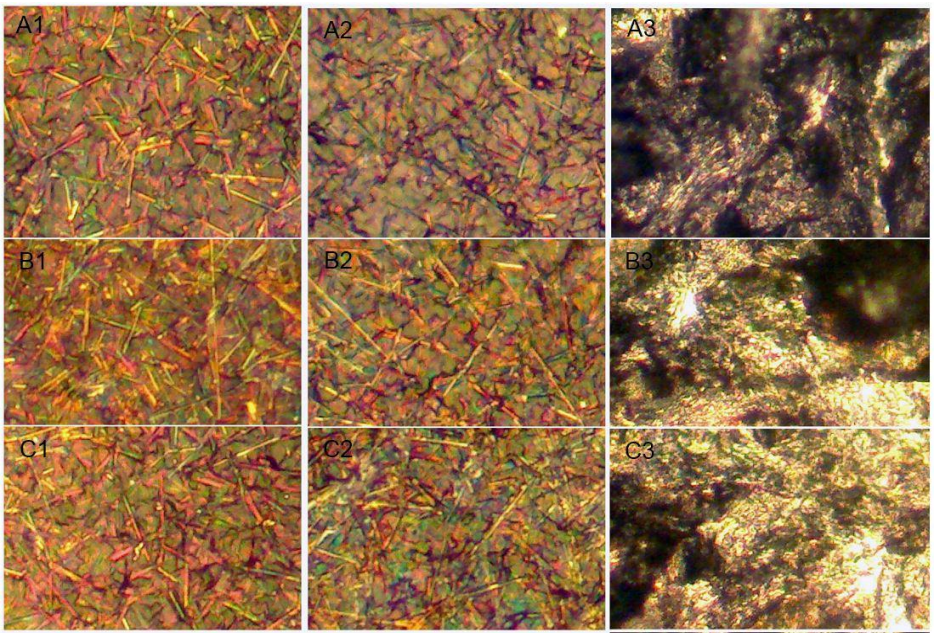

Figure 4-9. Optical images of 3% AgNW before thermal curing (A1), after thermal curing (A2), after scribing (A3).6% AgNW before thermal curing (B1) after thermal Curing (B2), after scribing (B3). 9% AgNW before thermal curing (C1) after thermal Curing (C2),after scribing (C3).

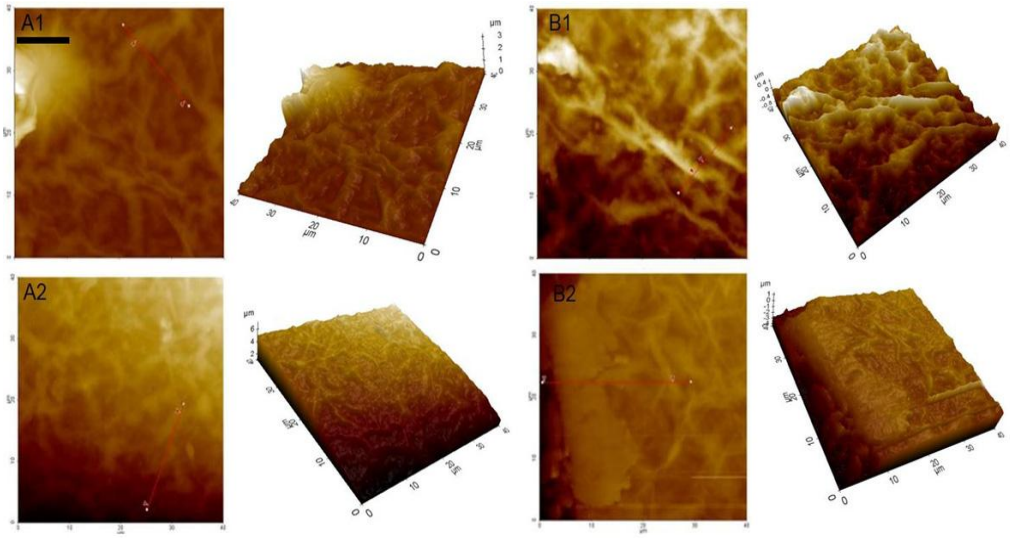

Figure 4-10. AFM images of 1% AgNW before thermal curing (A1), after thermal curing (A2), 1.5% AgNW before thermal curing (B1) after thermal Curing (B2). The black bar scale is 10 µm.

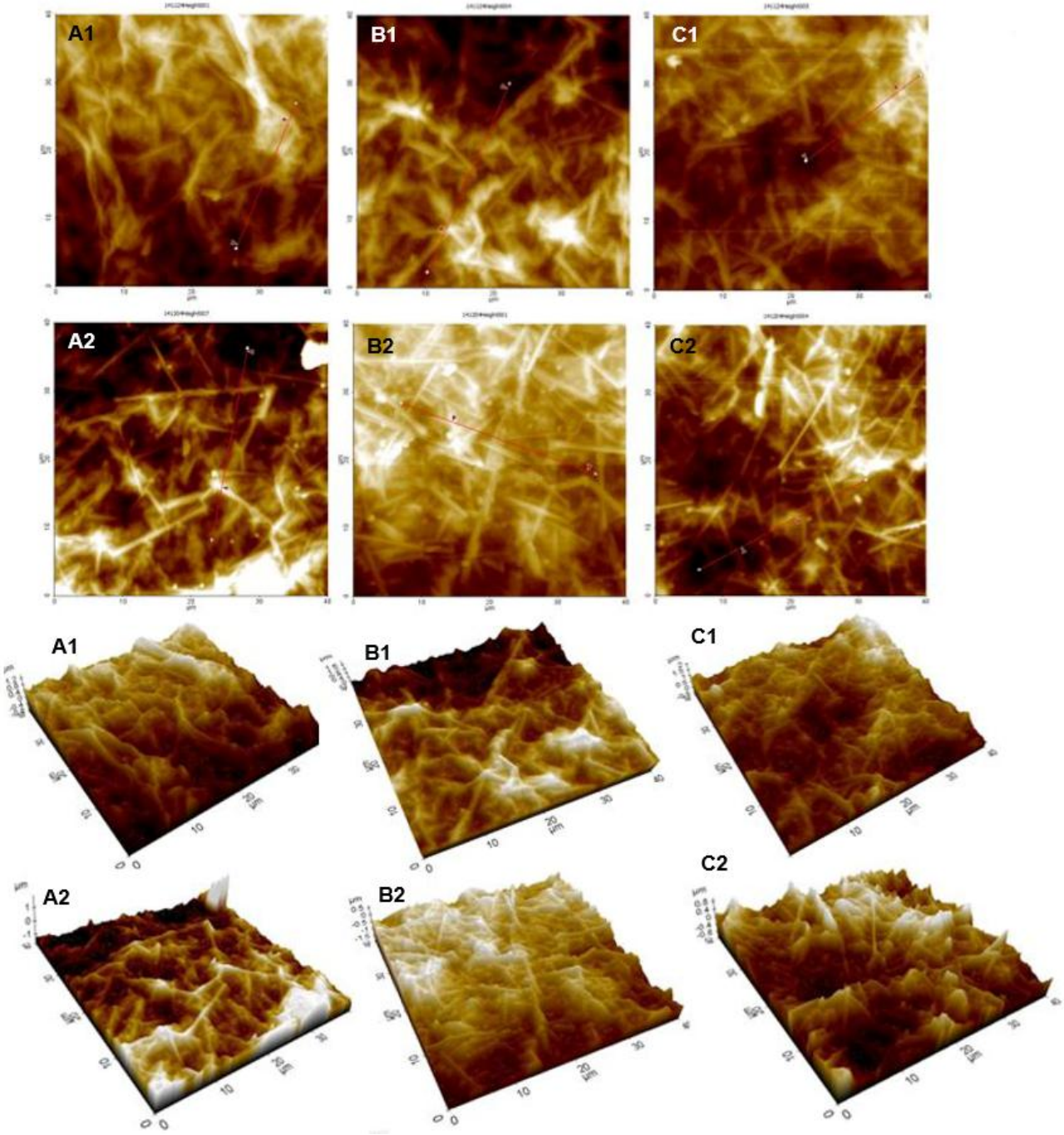

Figure 4-11. AFM images of 3% AgNW before thermal curing (A1), after thermal curing (A2), 6% AgNW before thermal curing (B1) after thermal Curing (B2), 9% AgNW before thermal curing (C1) after thermal Curing (C2).

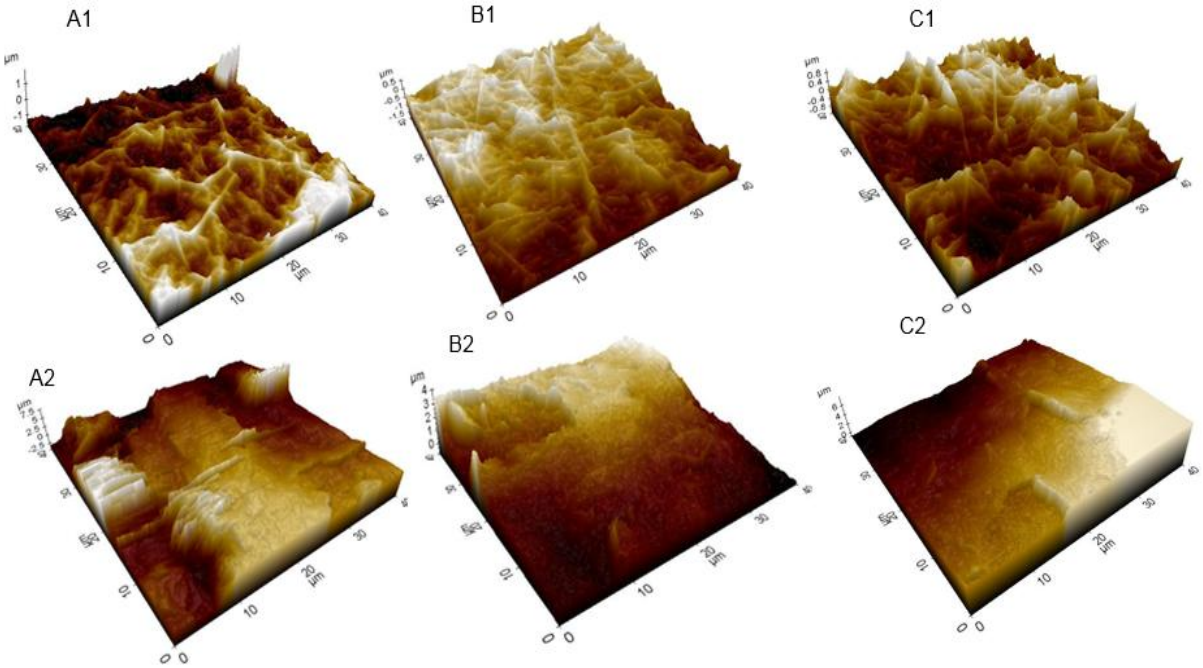

Figure 4-12. AFM images comparing before (A1) and after scribing for 3% AgNW (A2), before (B1) and after scribing for 6% AgNW (B2), before (C1) and after scribing for 9% AgNW (C2).

SEM images of hybrid thin film are shown in Figure 4-4. The scribed and un-scribed parts are totally different and recognizable. The images suggest that there are very few or no AgNWs in the scribed area. For non-scribed area, silver nano wires are completely visible, but after scribing it is almost impossible to see those wires. Figure 4-13 shows schematic of before and after scribing of hybrid layer. The laser beam reduces the GO by removing oxygen groups and also thermal expansion causes the displacement of layers of r-GO and those displaced layers cover the wires, so the random orientation of layers of r-GO, block the wires from the view.

4.3.3. EDX Analysis of Hybrid film

Figure 4-15 shows the EDX result for scribed and un-scribe hybrid layer. Hybrid samples show the removal of huge amount of oxygen from surface, Silver picks can be seen in both scribed and non-scribed ones slightly, but the quantity of silver in EDX is not enough to conclude that if the silver content is more or less in scribed part than un-scribed area.

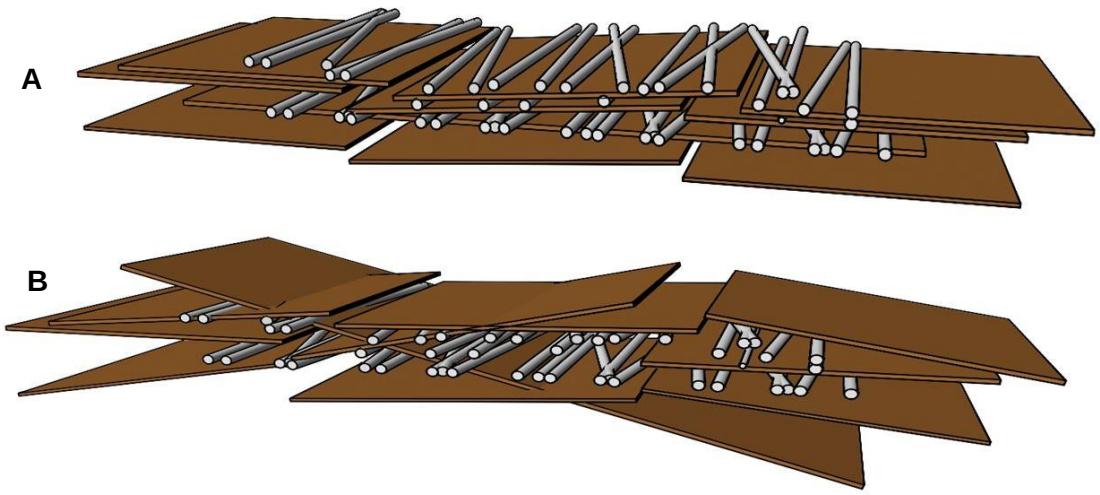

Figure 4-13. Schematic of hybrid structure before (A) and after scribing (B).

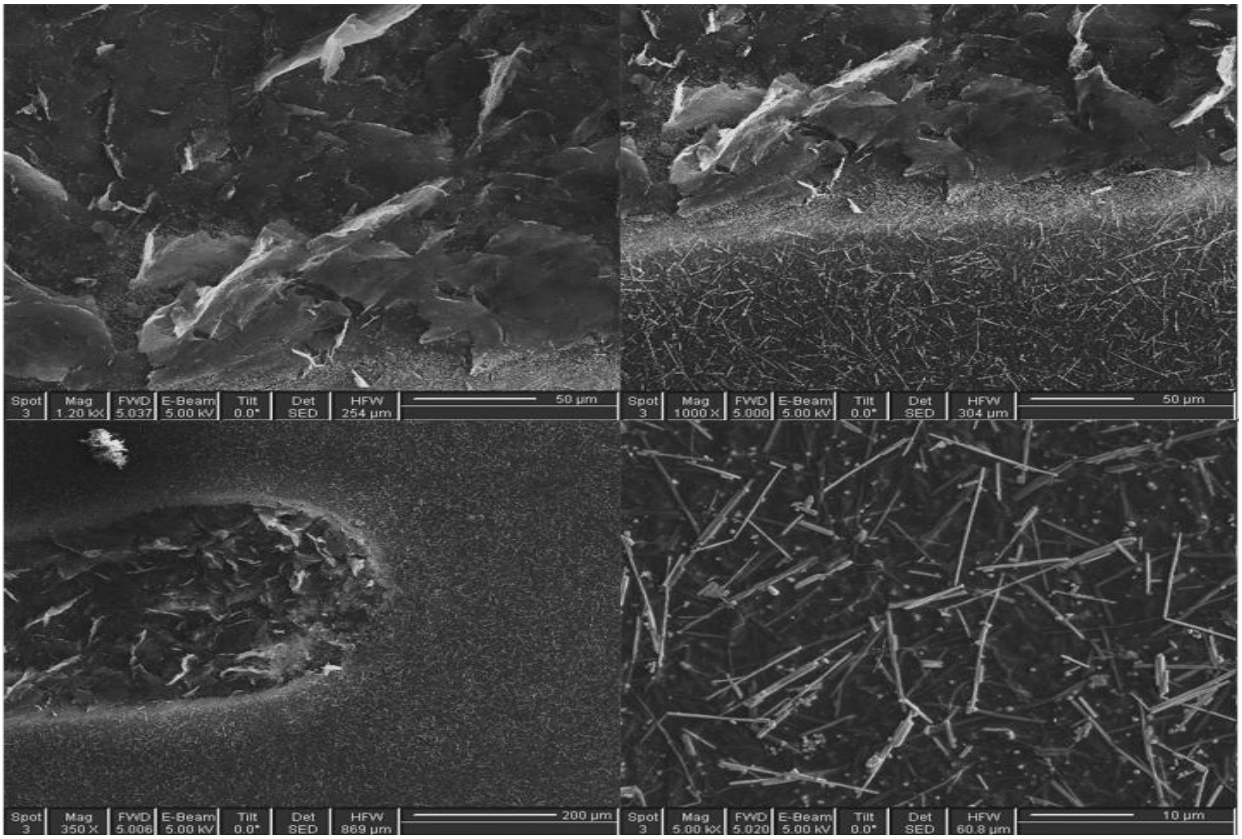

Figure 4-14. SEM images of 6% Hybrid sample.

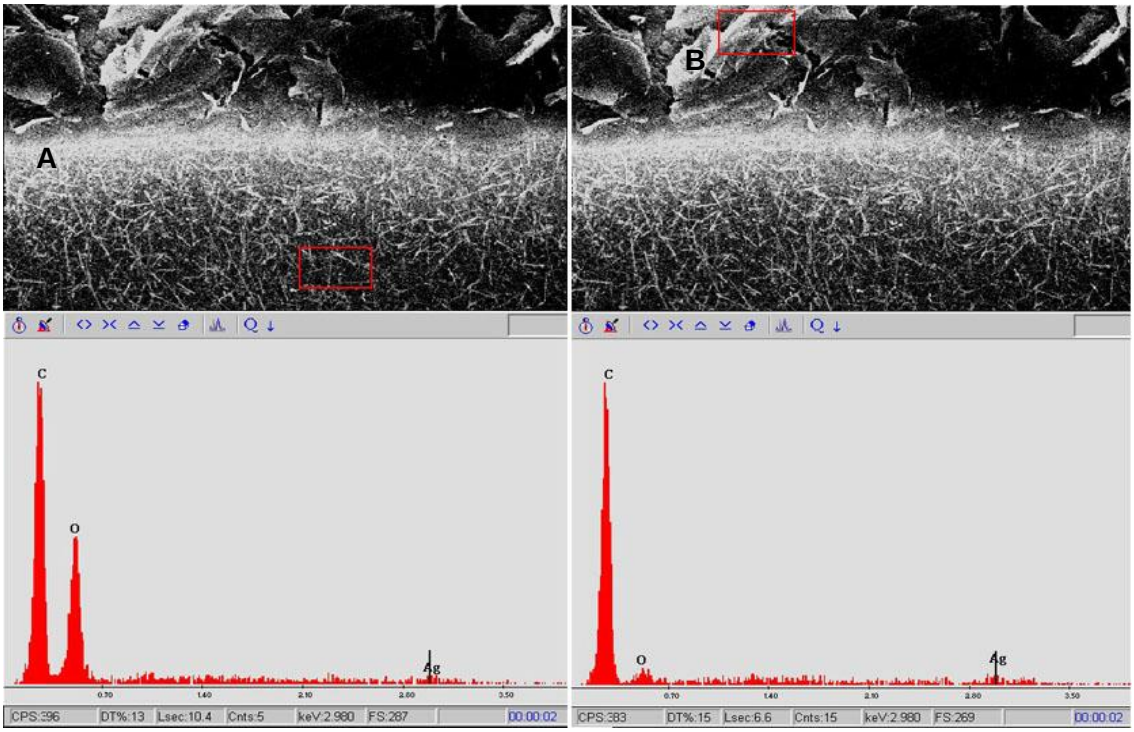

Figure 4-15. EDX images of 6% sample un-scribed area (A) and scribed area (B).

4.4. Characterization of Graphene Sensors

4.4.1. Temperature Sensor (resistance measurement)

Different temperatures from room temperature to 40°C are changed to see the sensor responses. A hot plate with controllable temperature is used as heat source and actual temperatures is checked by thermometer. Three sensors have been selected to check the resistivity changes and an AMPROBE 33XR-A multi meter is used to measure the resistance at different temperatures. Figure 4-16 shows that the resistivity of r-GO is decreased by increasing the temperature. The test has been done twice in two different days (48 hours difference), and the result shows no major changes in resistance. Eq. (4) **Error! Reference source not found.** is used to calculate resistance temperature coefficient (RTC). In this formula, R (T_0) is the resistance at room temperature (25°C) and α is RTC. According to the calculations RTC for r-GO found to be negative which is in agreement with previous reports [79], [80], [96].

Average value of α for different sensors shows a variation from -0.0024 to -0.00933 k^{-1} which is similar to characteristics of bi-layer Graphene and few layers Graphene [79]. Therefore we can expect that a combination of different numbers of layers can be obtained by laser scribing. It means that GO is reduced to r-GO successfully and not only monolayer of Graphene is produced but also multi-layer of Graphene is obtained.

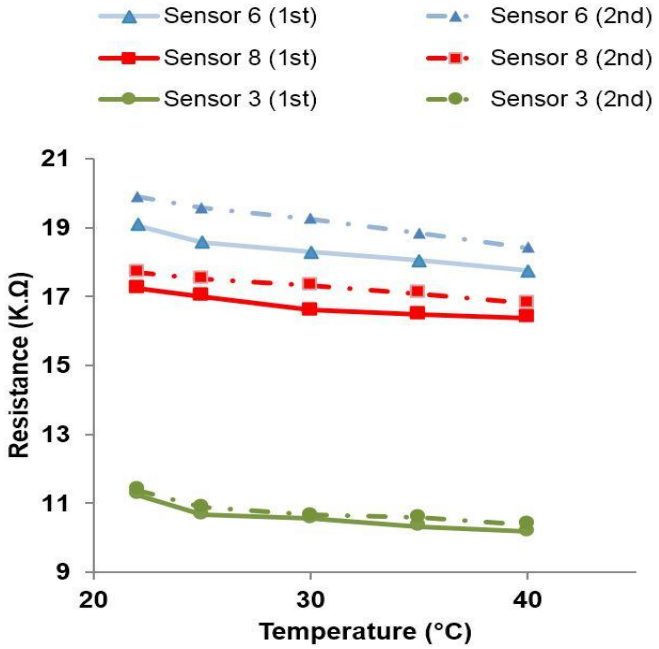

Figure 4-16. Resistance vs. Temperature for three Graphene-Based sensors.

4.4.2. Touch Sensor

A digital force gauge (Dillon Model GS) with hand wheel test stand is used to apply exact amount of pressure on sensors from 50 mN up to 500 mN (Figure 4-17 B). Finally the applied force is converted to pressure. An AMPROBE 33XR-A multi meter is used to record the voltage changes. Ideal touch sensors are designed to be linear depending on applied pressure. The pressure vs. voltage shows a linear dependency (Figure 4-18), which is desirable for touch sensor applications. Figure 4-17A shows the actual sensors.

The touch sensor also has been tested by touching sensors by slightly pressing them. In time intervals (10 seconds steps) by pressing and releasing the force several

times to see the piezo-resistive response (Figure 4-17 C). As graph shows, pressing and releasing the force changes the resistivity by increasing the contacts between Graphene layers, allowing more conductive paths for electrons which change the voltage consequently. This performance is reversible so the sensor restored to its initial status with little degradation. The harder sensors are pressed, the bigger voltage change is obtained (Figure 4-17). Pseudo piezo-resistive mechanism of the fabricated sensor can be explained by the resistance change caused by the variation of the contacts among adjacent Graphene sheets while pressing the surface of the sensor. The scribed r-GO contains many Graphene sheets close to each other, by applying force on top of this structure the contact area between these sheets increases which leads to higher conductivity which is described in previous works [76]. Sensitivity of this particular sensor is about 19mV/kPa obtained by curve fitting and using the circuit shown in Figure 4-17D. Other works suggest that resistance change of Graphene structures is highly sensitive to macro-deformation or micro-defects. Therefore touch sensor application with r-GO is very promising [97].

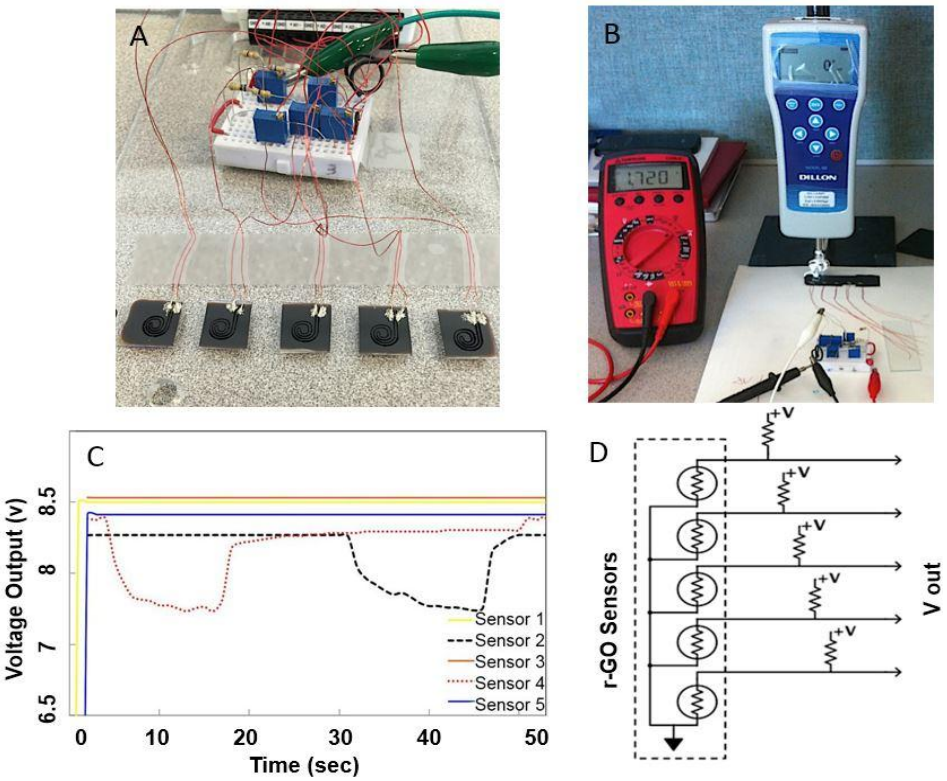

Figure 4-17. Schematics of 5 sesnor (A) test setup (B) Output response after touching (C) simple circuit design (D).

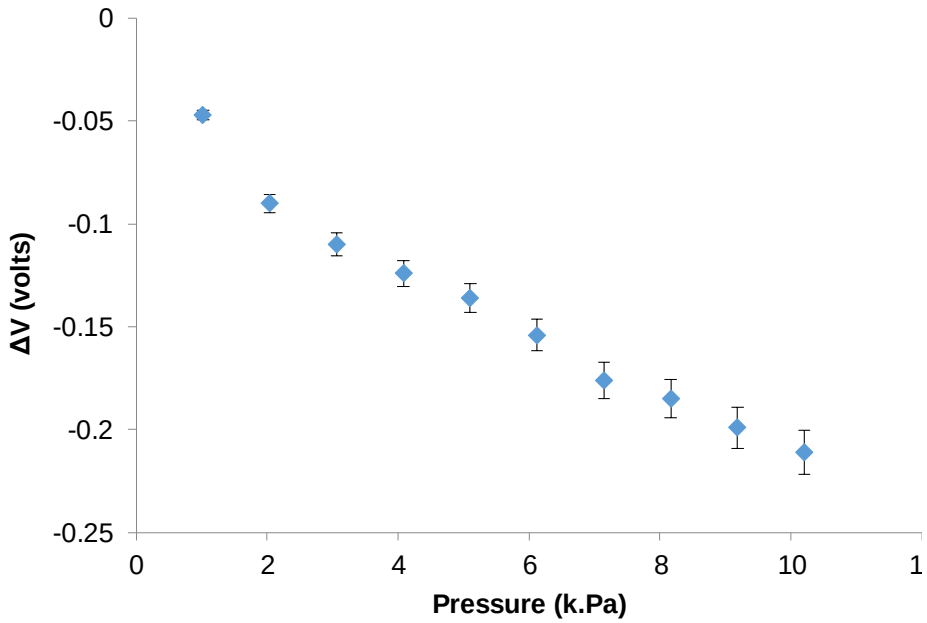

Figure 4-18. ΔV vs. Applied Pressure.

4.4.3. Hybrid Graphene Touch Sensor

Hybrid layer is scribed by laser to form a capacitor, to see its ability to be used as capacitor. This capacitor is a little bigger than human fingertip. Figure 4-19 depicted the design of this capacitor.

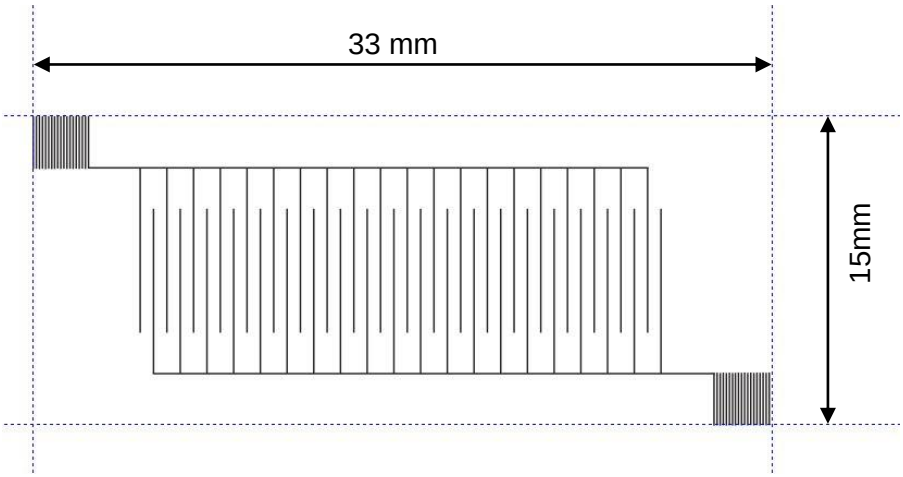

Figure 4-19. Schematic of Capacitor scribed on Hybrid film.

Capacitance easily can be changed by mechanical touch on the capacitor surface. Repeated touch and release with more than 30 times didn't change the

capacitance values significantly. Therefore the capacitance change has been reliably detected. Samples are indicated based on their AgNW content from 3 to 9% and results are summarized in Table 4-3. The capacitance values are measured using LCR machine. From the table, sample with 9% AgNW shows higher change in capacitance among three samples. Although the changes in capacitance are 2 order of magnitude but it is in detectable range.

Table 4-3. Capacitance changes of hybrid layer before and after touching

Hybrid Sample	3% (AgNW)	6% (AgNW)	9% (AgNW)
Initial capacitance	11.3pf	12.4pf	51pf
After touch capacitance	200pf	210pf	500pf

Figure 4-20 shows the actual capacitor which is a thin film hybrid of Silver nano wire (6%) and GO and patterned with laser.

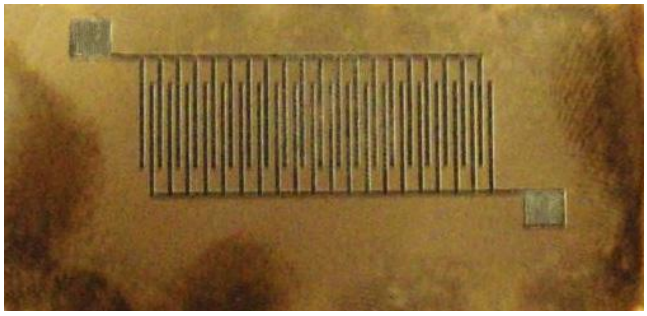

Figure 4-20. Schematic of fabricated capacitor using hybrid thin film.

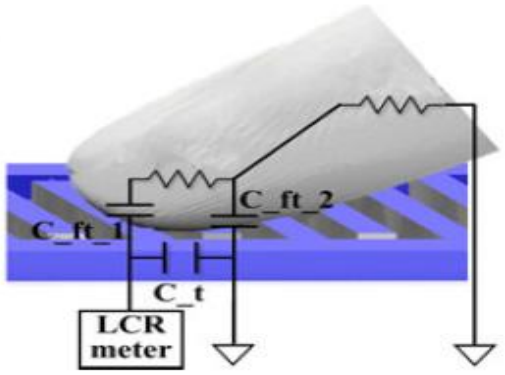

Figure 4-21. Schematic of capacitance change after touching [97]. Reprinted with permission.

Changes in resistance of hybrid film after being touched can make touch sensor's capacitance changed significantly. In addition to pseudo piezo-resistive mechanism, capacitance between the finger and the inter-digitated electrode (IDE) can change. Human finger acts like an electrolyte, and capacitance between the finger and the IDE changes. When the finger touches the IDE, capacitances of finger (C_ft_1 and C_ft_2) add up to the initial capacitance of the (C_t) in parallel so that the resulting total capacitance increases and after removing the finger, the original capacitance is recovered (Figure 4-21). Others reported the fabrication of capacitance based on only silver nano particle and the initial and after touch capacitance are 25pF and 1000pF respectively [97].

Chapter 5

Conclusion and Future work

5.1. Conclusion

Manipulation of properties of GO and turn it into r-GO with better electrical conductivity using laser technology to fabricate sensors based on only Graphene can be useful as replacements for conventional sensors. This work describes a fast, simple and low cost method of reduction of GO. Reduction of GO film using laser technology (Chapter 3), fabrication of sensors as an application (Chapter 3), several analysis like optical and atomic microscopy, chemical analysis (FTIR, EDX) and electrical property measurement (Chapter 4) are done in this project to evaluate the final product.

We have shown that GO thin film can be reduced using laser beam successfully. Beside the laser scribing of thin film GO, chemical reduction of GO solution using hydrazine is tried but the quality of final r-GO is poor and not applicable for making thin film and sensor, also it is chemical based and needs to deal with solution and sometimes toxic substance which is less desirable.

Other method of thin film fabrication is tried. Spraying the GO solution with air brush or spraying of mixture of GO and silver nano wire shows that huge amount of precursor has been wasted, also this method leaves a lot of dirt and it is harmful due to spraying of metal nano wires. Spraying needs to be done under proper duct hood and it needs to be done with nitrogen in order to minimize to effect of oxidation on silver nano wires.

It is found that the thickness of thin film should be in micrometer range for the CO_2 laser scribing. Laser beam parameter such as power, speed, and distance to film surface is optimized in order to have best conductivity of reduced Graphene oxide.

Imaging techniques, FTIR and EDX analysis shows the morphology and chemical properties of surface and confirmed the reduction and removing of oxygen atoms from the surface.

As an application for this method of reduction, touch and temperature sensors are fabricated using laser patterning of thin film. It is shown that r-GO thin film has good sensitivity for using as touch sensor and the voltage vs. pressure is almost linear which is desirable for sensor applications. The fabricated device has shown reversibility for surface touch/pressure sensor applications. We believe that the high-sensitivity (19mV/kPa) of the r-GO touch sensors might be exploited in the wearable electronics and tactile sensing, as it is light and can conform to any surfaces. The touch sensor worked fine at the beginning but after several touches, the r-GO surface got damaged because it is fragile.

It has been shown that r-GO thin film has enough sensibility for using as temperature sensor. Resistance temperature coefficient is negative for Graphene and it is not a fixed number due to mixture of monolayer and few layers Graphene after laser scribing.

5.2. Future work

In some aspects, the final sensor can be improved by a fixing some technical issues.

- The quality of Graphene is very important and has major effect on final device. So instead of GO solution, other type of Graphene can be used.

- Other source of laser may have better final results, less power and lower speed can be tried using low power laser, like DVD writers.

- The surface of touch sensor is vulnerable to long time touching. It is very desirable to find a way to protect the surface from damaging and the durability can be increased a lot.

- Additional analytical techniques like TEM and high resolution SEM can reveal more details of Graphene layers before and after reduction.

- Laser interaction with Graphene, temperature distribution and electrical enhancement can be studied theoretically or by computer simulation and modeling.

References

[1] T. Sekitani and T. Someya, “Stretchable, Large-area Organic Electronics,” *Adv. Mater.*, vol. 22, no. 20, pp. 2228–2246, May 2010.

[2] A. K. Geim and K. S. Novoselov, “The rise of graphene,” *Nat. Mater.*, vol. 6, no. 3, pp. 183–191, Mar. 2007.

[3] A. H. Castro Neto, F. Guinea, N. M. R. Peres, K. S. Novoselov, and A. K. Geim, “The electronic properties of graphene,” *Rev. Mod. Phys.*, vol. 81, no. 1, pp. 109–162, Jan. 2009.

[4] K. S. Novoselov, V. I. Fal′ko, L. Colombo, P. R. Gellert, M. G. Schwab, and K. Kim, “A roadmap for graphene,” *Nature*, vol. 490, no. 7419, pp. 192–200, Oct. 2012.

[5] S. Mikhailov, Ed., *Physics and Applications of Graphene - Experiments*. InTech, 2011.

[6] T. Enoki and T. Ando, *Physics and Chemistry of Graphene: Graphene to Nanographene*. CRC Press, 2013.

[7] A. Reina, X. Jia, J. Ho, D. Nezich, H. Son, V. Bulovic, M. S. Dresselhaus, and J. Kong, “Large Area, Few-Layer Graphene Films on Arbitrary Substrates by Chemical Vapor Deposition,” *Nano Lett.*, vol. 9, no. 1, pp. 30–35, Jan. 2009.

[8] Y. Zhu, S. Murali, W. Cai, X. Li, J. W. Suk, J. R. Potts, and R. S. Ruoff, “Graphene and Graphene Oxide: Synthesis, Properties, and Applications,” *Adv. Mater.*, vol. 22, no. 35, pp. 3906–3924, Sep. 2010.

[9] G. Eda, G. Fanchini, and M. Chhowalla, “Large-area ultrathin films of reduced graphene oxide as a transparent and flexible electronic material,” *Nat. Nanotechnol.*, vol. 3, no. 5, pp. 270–274, May 2008.

[10] W. Walukiewicz, L. Lagowski, L. Jastrzebski, M. Lichtensteiger, and H. C. Gatos, “Electron mobility and free-carrier absorption in GaAs: Determination

of the compensation ratio," *J. Appl. Phys.*, vol. 50, no. 2, pp. 899–908, Feb. 1979.

[11] J. J. Wortman and R. A. Evans, "Young's Modulus, Shear Modulus, and Poisson's Ratio in Silicon and Germanium," *J. Appl. Phys.*, vol. 36, no. 1, pp. 153–156, Jan. 1965.

[12] B. E. Sernelius, K.-F. Berggren, Z.-C. Jin, I. Hamberg, and C. G. Granqvist, "Band-gap tailoring of ZnO by means of heavy Al doping," *Phys. Rev. B*, vol. 37, no. 17, pp. 10244–10248, Jun. 1988.

[13] W. Cai, A. L. Moore, Y. Zhu, X. Li, S. Chen, L. Shi, and R. S. Ruoff, "Thermal Transport in Suspended and Supported Monolayer Graphene Grown by Chemical Vapor Deposition," *Nano Lett.*, vol. 10, no. 5, pp. 1645–1651, May 2010.

[14] M. Ruan, Y. Hu, Z. Guo, R. Dong, J. Palmer, J. Hankinson, C. Berger, and W. A. de Heer, "Epitaxial graphene on silicon carbide: Introduction to structured graphene," *MRS Bull.*, vol. 37, no. 12, pp. 1138–1147, Dec. 2012.

[15] J. Chen, M. Duan, and G. Chen, "Continuous mechanical exfoliation of graphene sheets via three-roll mill," *J. Mater. Chem.*, vol. 22, no. 37, p. 19625, 2012.

[16] P. Song, X. Zhang, M. Sun, X. Cui, and Y. Lin, "Synthesis of graphene nanosheets via oxalic acid-induced chemical reduction of exfoliated graphite oxide," *RSC Adv.*, vol. 2, no. 3, p. 1168, 2012.

[17] H.-L. Guo, X.-F. Wang, Q.-Y. Qian, F.-B. Wang, and X.-H. Xia, "A Green Approach to the Synthesis of Graphene Nanosheets," *ACS Nano*, vol. 3, no. 9, pp. 2653–2659, 2009.

[18] D. A. Sokolov, K. R. Shepperd, and T. M. Orlando, "Formation of Graphene Features from Direct Laser-Induced Reduction of Graphite Oxide," *J. Phys. Chem. Lett.*, vol. 1, no. 18, pp. 2633–2636, 2010.

[19] A. Ismach, C. Druzgalski, S. Penwell, A. Schwartzberg, M. Zheng, A. Javey, J. Bokor, and Y. Zhang, "Direct Chemical Vapor Deposition of Graphene on Dielectric Surfaces," *Nano Lett.*, vol. 10, no. 5, pp. 1542–1548, 2010.

[20] J. Coraux, A. T. N'Diaye, M. Engler, C. Busse, D. Wall, N. Buckanie, F.-J. M. zu Heringdorf, R. van Gastel, B. Poelsema, and T. Michely, "Growth of graphene on Ir(111)," *New J. Phys.*, vol. 11, no. 2, p. 023006, Feb. 2009.

[21] Y. Zhang, L. Zhang, and C. Zhou, “Review of Chemical Vapor Deposition of Graphene and Related Applications,” *Acc. Chem. Res.*, vol. 46, no. 10, pp. 2329–2339, 2013.

[22] X. Li, W. Cai, J. An, S. Kim, J. Nah, D. Yang, R. Piner, A. Velamakanni, I. Jung, E. Tutuc, S. K. Banerjee, L. Colombo, and R. S. Ruoff, “Large-Area Synthesis of High-Quality and Uniform Graphene Films on Copper Foils,” *Science*, vol. 324, no. 5932, pp. 1312–1314, Jun. 2009.

[23] “Chem. Vap. Deposition (1–2–3/2015),” *Chem. Vap. Depos.*, vol. 21, no. 1–2–3, p. n/a–n/a, Mar. 2015.

[24] “http://www.azom.com/article.aspx?ArticleID=1552.” .

[25] M. Losurdo, M. M. Giangregorio, P. Capezzuto, and G. Bruno, “Graphene CVD growth on copper and nickel: role of hydrogen in kinetics and structure,” *Phys. Chem. Chem. Phys.*, vol. 13, no. 46, pp. 20836–20843, Nov. 2011.

[26] L. Huang, Q. H. Chang, G. L. Guo, Y. Liu, Y. Q. Xie, T. Wang, B. Ling, and H. F. Yang, “Synthesis of high-quality graphene films on nickel foils by rapid thermal chemical vapor deposition,” *Carbon*, vol. 50, no. 2, pp. 551–556, Feb. 2012.

[27] X. Li, Y. Zhu, W. Cai, M. Borysiak, B. Han, D. Chen, R. D. Piner, L. Colombo, and R. S. Ruoff, “Transfer of Large-Area Graphene Films for High-Performance Transparent Conductive Electrodes,” *Nano Lett.*, vol. 9, no. 12, pp. 4359–4363, 2009.

[28] Y. Hernandez, V. Nicolosi, M. Lotya, F. M. Blighe, Z. Sun, S. De, I. T. McGovern, B. Holland, M. Byrne, Y. K. Gun’Ko, J. J. Boland, P. Niraj, G. Duesberg, S. Krishnamurthy, R. Goodhue, J. Hutchison, V. Scardaci, A. C. Ferrari, and J. N. Coleman, “High-yield production of graphene by liquid-phase exfoliation of graphite,” *Nat. Nanotechnol.*, vol. 3, no. 9, pp. 563–568, Sep. 2008.

[29] V. Skakalova and A. B. Kaiser, Eds., *Graphene: Properties, Preparation, Characterisation and Devices*, 1 edition. Cambridge ; Waltham, MA: Woodhead Publishing, 2014.

[30] C. K. Chua and M. Pumera, “Chemical reduction of graphene oxide: a synthetic chemistry viewpoint,” *Chem. Soc. Rev.*, vol. 43, no. 1, pp. 291–312, Dec. 2013.

[31] S. Stankovich, D. A. Dikin, G. H. B. Dommett, K. M. Kohlhaas, E. J. Zimney, E. A. Stach, R. D. Piner, S. T. Nguyen, and R. S. Ruoff, “Graphene-based composite materials,” Nature, vol. 442, no. 7100, pp. 282–286, Jul. 2006.

[32] B. C. Brodie, “On the Atomic Weight of Graphite,” *Philos. Trans. R. Soc. Lond.*, vol. 149, pp. 249–259, Jan. 1859.

[33] W. S. Hummers and R. E. Offeman, “Preparation of Graphitic Oxide,” *J. Am. Chem. Soc.*, vol. 80, no. 6, pp. 1339–1339, Mar. 1958.

[34] L. J. Cote, F. Kim, and J. Huang, “Langmuir−Blodgett Assembly of Graphite Oxide Single Layers,” *J. Am. Chem. Soc.*, vol. 131, no. 3, pp. 1043–1049, Jan. 2009.

[35] D. C. Marcano, D. V. Kosynkin, J. M. Berlin, A. Sinitskii, Z. Sun, A. Slesarev, L. B. Alemany, W. Lu, and J. M. Tour, “Improved Synthesis of Graphene Oxide,” *ACS Nano*, vol. 4, no. 8, pp. 4806–4814, Aug. 2010.

[36] S. Stankovich, D. A. Dikin, R. D. Piner, K. A. Kohlhaas, A. Kleinhammes, Y. Jia, Y. Wu, S. T. Nguyen, and R. S. Ruoff, “Synthesis of graphene-based nanosheets via chemical reduction of exfoliated graphite oxide,” *Carbon*, vol. 45, no. 7, pp. 1558–1565, Jun. 2007.

[37] H.-J. Shin, K. K. Kim, A. Benayad, S.-M. Yoon, H. K. Park, I.-S. Jung, M. H. Jin, H.-K. Jeong, J. M. Kim, J.-Y. Choi, and Y. H. Lee, “Efficient Reduction of Graphite Oxide by Sodium Borohydride and Its Effect on Electrical Conductance,” *Adv. Funct. Mater.*, vol. 19, no. 12, pp. 1987–1992, Jun. 2009.

[38] W. Chen, L. Yan, and P. R. Bangal, “Chemical Reduction of Graphene Oxide to Graphene by Sulfur-Containing Compounds,” *J. Phys. Chem. C*, vol. 114, no. 47, pp. 19885–19890, Dec. 2010.

[39] D. Yang, A. Velamakanni, G. Bozoklu, S. Park, M. Stoller, R. D. Piner, S. Stankovich, I. Jung, D. A. Field, C. A. Ventrice Jr., and R. S. Ruoff, “Chemical analysis of graphene oxide films after heat and chemical treatments by X-ray photoelectron and Micro-Raman spectroscopy,” *Carbon*, vol. 47, no. 1, pp. 145–152, Jan. 2009.

[40] O. Akhavan, “The effect of heat treatment on formation of graphene thin films from graphene oxide nanosheets,” *Carbon*, vol. 48, no. 2, pp. 509–519, Feb. 2010.

[41] W. Chen, L. Yan, and P. R. Bangal, “Preparation of graphene by the rapid and mild thermal reduction of graphene oxide induced by microwaves,” *Carbon*, vol. 48, no. 4, pp. 1146–1152, Apr. 2010.

[42] Z. Lin, Y. Yao, Z. Li, Y. Liu, Z. Li, and C.-P. Wong, “Solvent-Assisted Thermal Reduction of Graphite Oxide,” *J. Phys. Chem. C*, vol. 114, no. 35, pp. 14819–14825, Sep. 2010.

[43] M. Zhang and Z. Wang, “Nanostructured silver nanowires-graphene hybrids for enhanced electrochemical detection of hydrogen peroxide,” *Appl. Phys. Lett.*, vol. 102, no. 21, p. 213104, May 2013.

[44] I. Jurewicz, A. Fahimi, P. E. Lyons, R. J. Smith, M. Cann, M. L. Large, M. Tian, J. N. Coleman, and A. B. Dalton, “Insulator-Conductor Type Transitions in Graphene-Modified Silver Nanowire Networks: A Route to Inexpensive Transparent Conductors,” *Adv. Funct. Mater.*, vol. 24, no. 48, pp. 7580–7587, Dec. 2014.

[45] M.-S. Lee, K. Lee, S.-Y. Kim, H. Lee, J. Park, K.-H. Choi, H.-K. Kim, D.-G. Kim, D.-Y. Lee, S. Nam, and J.-U. Park, “High-Performance, Transparent, and Stretchable Electrodes Using Graphene–Metal Nanowire Hybrid Structures,” *Nano Lett.*, vol. 13, no. 6, pp. 2814–2821, Jun. 2013.

[46] I. N. Kholmanov, C. W. Magnuson, A. E. Aliev, H. Li, B. Zhang, J. W. Suk, L. L. Zhang, E. Peng, S. H. Mousavi, A. B. Khanikaev, R. Piner, G. Shvets, and R. S. Ruoff, “Improved Electrical Conductivity of Graphene Films Integrated with Metal Nanowires,” *Nano Lett.*, vol. 12, no. 11, pp. 5679–5683, Nov. 2012.

[47] J. Liang, L. Li, K. Tong, Z. Ren, W. Hu, X. Niu, Y. Chen, and Q. Pei, “Silver Nanowire Percolation Network Soldered with Graphene Oxide at Room Temperature and Its Application for Fully Stretchable Polymer Light-Emitting Diodes,” *ACS Nano*, vol. 8, no. 2, pp. 1590–1600, Feb. 2014.

[48] K. Naito, N. Yoshinaga, E. Tsutsumi, and Y. Akasaka, “Transparent conducting film composed of graphene and silver nanowire stacked layers,” *Synth. Met.*, vol. 175, pp. 42–46, Jul. 2013.

[49] B. W. An, B. G. Hyun, S.-Y. Kim, M. Kim, M.-S. Lee, K. Lee, J. B. Koo, H. Y. Chu, B.-S. Bae, and J.-U. Park, “Stretchable and Transparent Electrodes using Hybrid Structures of Graphene–Metal Nanotrough Networks with High Performances and Ultimate Uniformity,” *Nano Lett.*, vol. 14, no. 11, pp. 6322–6328, Nov. 2014.

[50] H.-W. Tien, S.-T. Hsiao, W.-H. Liao, Y.-H. Yu, F.-C. Lin, Y.-S. Wang, S.-M. Li, and C.-C. M. Ma, “Using self-assembly to prepare a graphene-silver nanowire hybrid film that is transparent and electrically conductive,” *Carbon*, vol. 58, pp. 198–207, Jul. 2013.

[51] C. Xu, X. Wang, and J. Zhu, “Graphene−Metal Particle Nanocomposites,” *J. Phys. Chem. C*, vol. 112, no. 50, pp. 19841–19845, Dec. 2008.

[52] J. Feng, W. Li, X. Qian, J. Qi, L. Qi, and J. Li, “Patterning of graphene,” *Nanoscale*, vol. 4, no. 16, pp. 4883–4899, Jul. 2012.

[53] D. Wei and Y. Liu, “Controllable Synthesis of Graphene and Its Applications,” *Adv. Mater.*, vol. 22, no. 30, pp. 3225–3241, Aug. 2010.

[54] M. J. Allen, V. C. Tung, and R. B. Kaner, “Honeycomb Carbon: A Review of Graphene,” *Chem. Rev.*, vol. 110, no. 1, pp. 132–145, Jan. 2010.

[55] Z. Shi, R. Yang, L. Zhang, Y. Wang, D. Liu, D. Shi, E. Wang, and G. Zhang, “Patterning Graphene with Zigzag Edges by Self-Aligned Anisotropic Etching,” *Adv. Mater.*, vol. 23, no. 27, pp. 3061–3065, Jul. 2011.

[56] L. Tapasztó, G. Dobrik, P. Lambin, and L. P. Biró, “Tailoring the atomic structure of graphene nanoribbons by scanning tunnelling microscope lithography,” *Nat. Nanotechnol.*, vol. 3, no. 7, pp. 397–401, Jul. 2008.

[57] M. C. Lemme, D. C. Bell, J. R. Williams, L. A. Stern, B. W. H. Baugher, P. Jarillo-Herrero, and C. M. Marcus, “Etching of Graphene Devices with a Helium Ion Beam,” *ACS Nano*, vol. 3, no. 9, pp. 2674–2676, Sep. 2009.

[58] L. Zhang, S. Diao, Y. Nie, K. Yan, N. Liu, B. Dai, Q. Xie, A. Reina, J. Kong, and Z. Liu, “Photocatalytic Patterning and Modification of Graphene,” *J. Am. Chem. Soc.*, vol. 133, no. 8, pp. 2706–2713, Mar. 2011.

[59] T. Kim, H. Kim, S. W. Kwon, Y. Kim, W. K. Park, D. H. Yoon, A.-R. Jang, H. S. Shin, K. S. Suh, and W. S. Yang, “Large-Scale Graphene Micropatterns via Self-Assembly-Mediated Process for Flexible Device Application,” *Nano Lett.*, vol. 12, no. 2, pp. 743–748, Feb. 2012.

[60] A. Dimiev, D. V. Kosynkin, A. Sinitskii, A. Slesarev, Z. Sun, and J. M. Tour, “Layer-by-Layer Removal of Graphene for Device Patterning,” *Science*, vol. 331, no. 6021, pp. 1168–1172, Mar. 2011.

[61] X. Liang, Y.-S. Jung, S. Wu, A. Ismach, D. L. Olynick, S. Cabrini, and J. Bokor, “Formation of Bandgap and Subbands in Graphene Nanomeshes

with Sub-10 nm Ribbon Width Fabricated via Nanoimprint Lithography," *Nano Lett.*, vol. 10, no. 7, pp. 2454–2460, Jul. 2010.

[62] V. Strong, S. Dubin, M. F. El-Kady, A. Lech, Y. Wang, B. H. Weiller, and R. B. Kaner, "Patterning and Electronic Tuning of Laser Scribed Graphene for Flexible All-Carbon Devices," *ACS Nano*, vol. 6, no. 2, pp. 1395–1403, Feb. 2012.

[63] F. Torrisi, T. Hasan, W. Wu, Z. Sun, A. Lombardo, T. S. Kulmala, G.-W. Hsieh, S. Jung, F. Bonaccorso, P. J. Paul, D. Chu, and A. C. Ferrari, "Inkjet-Printed Graphene Electronics," *ACS Nano*, vol. 6, no. 4, pp. 2992–3006, Apr. 2012.

[64] X. Liang, Z. Fu, and S. Y. Chou, "Graphene Transistors Fabricated via Transfer-Printing In Device Active-Areas on Large Wafer," *Nano Lett.*, vol. 7, no. 12, pp. 3840–3844, Dec. 2007.

[65] S.-K. Lee, B. J. Kim, H. Jang, S. C. Yoon, C. Lee, B. H. Hong, J. A. Rogers, J. H. Cho, and J.-H. Ahn, "Stretchable Graphene Transistors with Printed Dielectrics and Gate Electrodes," *Nano Lett.*, vol. 11, no. 11, pp. 4642–4646, Nov. 2011.

[66] C.-Y. Su, D. Fu, A.-Y. Lu, K.-K. Liu, Y. Xu, Z.-Y. Juang, and L.-J. Li, "Transfer printing of graphene strip from the graphene grown on copper wires," *Nanotechnology*, vol. 22, no. 18, p. 185309, May 2011.

[67] W. Gao, N. Singh, L. Song, Z. Liu, A. L. M. Reddy, L. Ci, R. Vajtai, Q. Zhang, B. Wei, and P. M. Ajayan, "Direct laser writing of micro-supercapacitors on hydrated graphite oxide films," *Nat. Nanotechnol.*, vol. 6, no. 8, pp. 496–500, Aug. 2011.

[68] E. Kymakis, C. Petridis, T. D. Anthopoulos, and E. Stratakis, "Laser-Assisted Reduction of Graphene Oxide for Flexible, Large-Area Optoelectronics," *IEEE J. Sel. Top. Quantum Electron.*, vol. 20, no. 1, pp. 106–115, Jan. 2014.

[69] M. F. El-Kady and R. B. Kaner, "Scalable fabrication of high-power graphene micro-supercapacitors for flexible and on-chip energy storage," *Nat. Commun.*, vol. 4, p. 1475, Feb. 2013.

[70] M. C. Lemme, T. J. Echtermeyer, M. Baus, and H. Kurz, "A Graphene Field-Effect Device," *IEEE Electron Device Lett.*, vol. 28, no. 4, pp. 282–284, Apr. 2007.

[71] S. S. Sabri, P. L. Lévesque, C. M. Aguirre, J. Guillemette, R. Martel, and T. Szkopek, “Graphene field effect transistors with parylene gate dielectric,” *Appl. Phys. Lett.*, vol. 95, no. 24, p. 242104, Dec. 2009.

[72] Y.-M. Lin, C. Dimitrakopoulos, K. A. Jenkins, D. B. Farmer, H.-Y. Chiu, A. Grill, and P. Avouris, “100-GHz Transistors from Wafer-Scale Epitaxial Graphene,” *Science*, vol. 327, no. 5966, pp. 662–662, Feb. 2010.

[73] S. Bae, H. Kim, Y. Lee, X. Xu, J.-S. Park, Y. Zheng, J. Balakrishnan, T. Lei, H. Ri Kim, Y. I. Song, Y.-J. Kim, K. S. Kim, B. Özyilmaz, J.-H. Ahn, B. H. Hong, and S. Iijima, “Roll-to-roll production of 30-inch graphene films for transparent electrodes,” *Nat. Nanotechnol.*, vol. 5, no. 8, pp. 574–578, Aug. 2010.

[74] J. Wu, H. A. Becerril, Z. Bao, Z. Liu, Y. Chen, and P. Peumans, “Organic solar cells with solution-processed graphene transparent electrodes,” *Appl. Phys. Lett.*, vol. 92, no. 26, p. 263302, Jun. 2008.

[75] X. Wang, L. Zhi, and K. Müllen, “Transparent, Conductive Graphene Electrodes for Dye-Sensitized Solar Cells,” *Nano Lett.*, vol. 8, no. 1, pp. 323–327, Jan. 2008.

[76] H.-B. Yao, J. Ge, C.-F. Wang, X. Wang, W. Hu, Z.-J. Zheng, Y. Ni, and S.-H. Yu, “A Flexible and Highly Pressure-Sensitive Graphene–Polyurethane Sponge Based on Fractured Microstructure Design,” *Adv. Mater.*, vol. 25, no. 46, pp. 6692–6698, Dec. 2013.

[77] Q. Sun, D. H. Kim, S. S. Park, N. Y. Lee, Y. Zhang, J. H. Lee, K. Cho, and J. H. Cho, “Transparent, Low-Power Pressure Sensor Matrix Based on Coplanar-Gate Graphene Transistors,” *Adv. Mater.*, vol. 26, no. 27, pp. 4735–4740, Jul. 2014.

[78] V. Sorkin and Y. W. Zhang, “Graphene-based pressure nano-sensors,” *J. Mol. Model.*, vol. 17, no. 11, pp. 2825–2830, Feb. 2011.

[79] H. Al-Mumen, F. Rao, L. Dong, and W. Li, “Design, fabrication, and characterization of graphene thermistor,” in *2013 8th IEEE International Conference on Nano/Micro Engineered and Molecular Systems (NEMS)*, 2013, pp. 1135–1138.

[80] D. Kong, L. T. Le, Y. Li, J. L. Zunino, and W. Lee, “Temperature-Dependent Electrical Properties of Graphene Inkjet-Printed on Flexible Materials,” *Langmuir*, vol. 28, no. 37, pp. 13467–13472, Sep. 2012.

[81] V. Skákalová, A. B. Kaiser, J. S. Yoo, D. Obergfell, and S. Roth, “Correlation between resistance fluctuations and temperature dependence of conductivity in graphene,” *Phys. Rev. B*, vol. 80, no. 15, p. 153404, Oct. 2009.

[82] W.-P. Shih, L.-C. Tsao, C.-W. Lee, M.-Y. Cheng, C. Chang, Y.-J. Yang, and K.-C. Fan, “Flexible Temperature Sensor Array Based on a Graphite-Polydimethylsiloxane Composite,” *Sensors*, vol. 10, no. 4, pp. 3597–3610, Apr. 2010.

[83] P.-P. Zuo, H.-F. Feng, Z.-Z. Xu, L.-F. Zhang, Y.-L. Zhang, W. Xia, and W.-Q. Zhang, “Fabrication of biocompatible and mechanically reinforced graphene oxide-chitosan nanocomposite films,” *Chem. Cent. J.*, vol. 7, no. 1, p. 39, Feb. 2013.

[84] G. S. Nolas, J. Sharp, and H. J. Goldsmid, *Thermoelectrics: Basic Principles and New Materials Developments*. Springer Science & Business Media, 2001.

[85] C. Petridis, Y.-H. Lin, K. Savva, G. Eda, E. Kymakis, T. D. Anthopoulos, and E. Stratakis, “Post-fabrication, in situ laser reduction of graphene oxide devices,” *Appl. Phys. Lett.*, vol. 102, no. 9, p. 093115, Mar. 2013.

[86] Emerson Process Management, “Engineer’s Guide to Industrial Temperature Measurement.” © Emerson Electric Co. All rights reserved., 2013.

[87] C.-Y. Lee, G.-W. Wu, and W.-J. Hsieh, “Fabrication of micro sensors on a flexible substrate,” *Sens. Actuators Phys.*, vol. 147, no. 1, pp. 173–176, Sep. 2008.

[88] S. He, M. M. Mench, and S. Tadigadapa, “Thin film temperature sensor for real-time measurement of electrolyte temperature in a polymer electrolyte fuel cell,” *Sens. Actuators Phys.*, vol. 125, no. 2, pp. 170–177, Jan. 2006.

[89] R. C. Webb, A. P. Bonifas, A. Behnaz, Y. Zhang, K. J. Yu, H. Cheng, M. Shi, Z. Bian, Z. Liu, Y.-S. Kim, W.-H. Yeo, J. S. Park, J. Song, Y. Li, Y. Huang, A. M. Gorbach, and J. A. Rogers, “Ultrathin conformal devices for precise and continuous thermal characterization of human skin,” *Nat. Mater.*, vol. 12, no. 10, pp. 938–944, Oct. 2013.

[90] Y. Li, Y. Wu, and B. S. Ong, “Facile Synthesis of Silver Nanoparticles Useful for Fabrication of High-Conductivity Elements for Printed Electronics,” *J. Am. Chem. Soc.*, vol. 127, no. 10, pp. 3266–3267, Mar. 2005.

[91] J. Kim, K. Wubs, B.-S. Bae, and W. S. Kim, “Direct stamping of silver nanoparticles toward residue-free thick electrode,” *Sci. Technol. Adv. Mater.*, vol. 13, no. 3, p. 035004, Jun. 2012.

[92] J. H. Lee, P. Lee, D. Lee, S. S. Lee, and S. H. Ko, “Large-Scale Synthesis and Characterization of Very Long Silver Nanowires via Successive Multistep Growth,” *Cryst. Growth Des.*, vol. 12, no. 11, pp. 5598–5605, Nov. 2012.

[93] C. Petridis, Y.-H. Lin, K. Savva, G. Eda, E. Kymakis, T. D. Anthopoulos, and E. Stratakis, “Post-fabrication, in situ laser reduction of graphene oxide devices,” *Appl. Phys. Lett.*, vol. 102, no. 9, p. 093115, Mar. 2013.

[92] J. Zhang, H. Yang, G. Shen, P. Cheng, J. Zhang, and S. Guo, “Reduction of graphene oxide via L-ascorbic acid,” *Chem. Commun.*, vol. 46, no. 7, pp. 1112–1114, Feb. 2010.

[95] L. Huang, Y. Liu, L.-C. Ji, Y.-Q. Xie, T. Wang, and W.-Z. Shi, “Pulsed laser assisted reduction of graphene oxide,” *Carbon*, vol. 49, no. 7, pp. 2431–2436, Jun. 2011.

[96] Y.-W. Tan, Y. Zhang, H. L. Stormer, and P. Kim, “Temperature dependent electron transport in graphene,” *Eur. Phys. J. Spec. Top.*, vol. 148, no. 1, pp. 15–18, Sep. 2007.

[97] J. Kim, J. H. Jong, and W. S. Kim, “Repeatedly Bendable Paper Touch Pad via Direct Stamping of Silver Nanoink With Pressure-Induced Low-Temperature Annealing,” *IEEE Trans. Nanotechnol.*, vol. 12, no. 6, pp. 1139–1143, Nov. 2013.